The Meteoritical Society

Meteoritics & Planetary Science 42, Nr 9, 1505–1527 (2007)
Abstract available online at http://meteoritics.org

Magnetic characterization of Cretaceous-Tertiary boundary sediments

Víctor VILLASANTE-MARCOS[1*], Francisca MARTÍNEZ-RUIZ[2], María Luisa OSETE[1], and Jaime URRUTIA-FUCUGAUCHI[3]

[1]Laboratorio de Paleomagnetismo, Departamento de Física de la Tierra, Astronomía y Astrofísica I, Facultad de CC. Físicas, Universidad Complutense de Madrid, Avda. Complutense, s/n, 28040 Madrid, Spain
[2]Instituto Andaluz de Ciencias de la Tierra (CSIC-UGR), Facultad de Ciencias, Campus Fuentenueva, 18002 Granada, Spain
[3]Instituto de Geofísica, Universidad Nacional Autónoma de México, Coyoacan 04510 D.F., Mexico
*Corresponding author. E-mail: vicvilla@fis.ucm.es

(Received 24 November 2006; revision accepted 19 February 2007)

Abstract–Rock magnetic properties across several K-T boundary sections have been investigated to reveal any possible magnetic signature associated with the remains of the impact event at the end of the Cretaceous. Studied sections' locations vary in distance to the Chicxulub structure from distal (Agost and Caravaca, Spain), through closer (ODP Hole 1049A, Blake Nose, North Atlantic), to proximal (El Mimbral and La Lajilla, Mexico). A clear magnetic signature is associated with the fireball layer in the most distal sections, consisting of a sharp increase in susceptibility and saturation isothermal remanent magnetization (SIRM), and a decrease in remanence coercivity. Magnetic properties in these sections point to a distinctive ferrimagnetic phase, probably corresponding to the reported Mg- and Ni-rich, highly oxidized spinels of meteoritic origin. At closer and proximal sections magnetic properties are different. Although there is an increase in susceptibility and SIRM associated with a rusty layer placed on top of the siliciclastic deposit in proximal sections, and with a similar limonitic layer on top of the spherule bed that defines the boundary at Blake Nose, the magnetic properties indicate a mixture of iron oxyhydroxides dominated by fine-grained goethite. Based on previous geochemical studies at Blake Nose and new geochemical and PGE abundance measurements performed in this work at El Mimbral, this goethite-rich layer can be interpreted as an effect of diagenetic remobilization and precipitation of Fe. There is not enough evidence to assert that this Fe concentration layer at proximal sections is directly related to deposition of fine meteoritic material. Magnetic, geochemical, and iridium data reject it as a primary meteoritic phase.

INTRODUCTION

Since 1980, when the anomalous abundance of iridium at K-T boundary sections around the world was first noticed (Alvarez et al. 1980; Smit and Hertogen 1980), great attention has been focused on the importance of meteorite impacts on the evolution of life. The simultaneity of the K-T boundary with the Chicxulub impact event is well established (Swisher et al. 1992; Sharpton et al. 1992). Over the years, an increasing quantity of information about the worldwide-distributed footprints of this impact has been accumulated. Among these footprints are geochemical anomalies, mainly high abundance of iridium and other platinum group elements (PGE) (Alvarez et al. 1980; Smit and Hertogen 1980; Kyte et al. 1980; Ganapathy 1980; Kyte 2002; Claeys et al. 2002); presence of minerals with features corresponding to ultrahigh pressure (shock) deformation (Bohor et al. 1984, 1987; Claeys et al. 2002); Os- and Cr-isotopic anomalies (Turekian 1982; Luck and Turekian 1983; Shukolyukov and Lugmair 1998); tektites, microtektites, and microkrystites with varying degrees of postdepositional alteration (Smit and Klaver 1981; Montanari et al. 1983; Smit and Kyte 1984; Sigurdsson et al. 1991; Smit et al. 1992; Kyte 2002); and presence of magnesium and nickel-rich spinels (Smit and Kyte 1984; Kyte and Smit 1986; Robin et al. 1992; Kyte and Bostwick 1995). These advances in K-T boundary event investigation have been made in correlation with the findings in a more general subject: the discovery and characterization of impact markers in the stratigraphic record.

The application of rock magnetism as a tool in K-T boundary studies was first performed by Worm and Banerjee (1987) in their study of the Petriccio section (Italy) and five DSDP sections in western Pacific and Indian oceans. In Petriccio, these authors measured several magnetic

parameters both on bulk sample and on a set of microspherules magnetically extracted from the K-T boundary clay. The magnetic signal of this layer was found to be concentrated in the microspherules, and hysteresis, thermomagnetic, and isothermal remanent magnetization (IRM) results were interpreted as proof of a close-to-magnetite composition of the skeletal ferrites contained in the microspherules. A multidomain behavior was also deduced. Regarding the DSDP sites, core surface susceptibility was measured and sharp increases were found in connection with the K-T boundary layer, although in some cases the magnetic peak was displaced with respect to the iridium spike.

Cisowski (1988, 1990) also used magnetic properties to study five highly magnetic microspherules from the Petriccio K-T boundary section and in bulk samples from both marine (Petriccio and Gubbio, Italy) and continental K-T boundary sections (Starkville South, Brownie Butte, and Glendive, USA). According to the IRM acquisition and demagnetization patterns, as well as the thermomagnetic and low-temperature measurements, the author concluded that the magnetic properties of the spherules were consistent with the previously reported presence of skeletal magnesioferrites with varying degrees of cation substitution. In agreement with the results of Worm and Banerjee (1987), the magnetic properties of the bulk clay samples could be explained simply by dissolution of magnetic spherules (with embedded magnesioferrite grains) in a less magnetic matrix. But, in contrast to Worm and Banerjee results, Cisowski did not find close to magnetite thermomagnetic behavior, even when the samples came from the same section. This fact could be explained by differences in the spherule extraction methods. While Cisowski hand-picked the spherules individually, Worm and Banerjee performed magnetic extraction, and a bias toward phases with higher saturation magnetization (and hence toward magnetite-like phases) could exist in their samples.

Morden (1993) conducted rock magnetic experiments in the K-T boundary Fish Clay of Stevns Klint (Denmark), both in bulk sample and in a magnetic extraction. The Curie curves of the magnetic extraction showed the presence of some Fe particles with low Ni-content, and the authors interpreted it as low-Ni iron spherules originated from the vaporized K-T impactor.

Griscom et al. (1999) have applied electron spin resonance to investigate the magnetic mineralogy of K-T boundary material. These authors reported anomalous increases of ferromagnetic resonance intensity (FMR) just at the K-T boundary layer in Caravaca and Sopelana (Spain) and Gubbio (Italy) sections. The FMR intensities and their dependence on temperature were interpreted as indicating the presence of spherical fine-grained magnetite particles. The size of these particles was determined to be 4.6 nm by means of fitting the FMR temperature-dependent behavior to theoretical calculations for spherical single-domain–magnetite particles. The authors interpreted this magnetic phase to have not an extraterrestrial origin, but to come from weathered glass spherules produced by the Chicxulub impact from the target material. After distribution and deposition, this glass would transform to clay, but the magnetite particles pervading it would survive. This interpretation was based on detecting similar phases in Beloc glass tektites and Chicxulub melt rock coming from PEMEX Y6-N19 drill core. The authors reported also the presence of goethite in Gubbio K-T boundary layer, but did not find similar results for Caravaca. Moreover, the authors described their technique as insensitive to multidomain magnetic phases. In that way, the absence of any signal coming from the magnesium and nickel-rich spinels previously detected in the K-T boundary layer was explained, regarding that the authors expected multidomain behavior for these spinels because their reported sizes were greater than 1 micron.

Brooks et al. (1985) used X-ray diffraction and Mössbauer spectroscopy to analyze bulk sample and iron oxide spheroids from the basal K-T boundary layer at Woodside Creek (New Zealand). They identified microcrystalline goethite (10–20 nm) in the matrix and crystalline goethite (>200 nm) and some hematite in the spheroids. Based on geochemical data, the authors interpreted these magnetic phases as authigenic products, probably formed from pyrite clumps originated in the very reducing post-impact environment.

Wdowiak et al. (2001) have recently used Mössbauer spectroscopy in several K-T boundary sections. These measurements were performed exclusively on samples from what the authors described as the fireball layer in El Mimbral and Bochil (Mexico), Moscow Landing, Starkville South, Madrid East, and Berwind Canyon (USA), Caravaca and Agost (Spain), Stevns Klint (Denmark), and Petriccio and Contessa (Gubbio, Italy). A ubiquitous and distinct magnetic phase was identified showing a superparamagnetic behavior at room temperature. In all investigated sections, except those at Gubbio, this phase is reported to be goethite with various particle sizes up to a few tens of nanometers, this result being also supported by X-ray diffraction. In the Italian sections, the superparamagnetic phase is interpreted as hematite. No magnetic order is detected at room temperature except in the Bochil, Contessa, and Petriccio sections. The authors report different sizes for this nanophase material depending on the geographic location, and point to the possibility that this nanophase could be the iridium K-T boundary carrier. Also, the authors suggest that this nanophase originated from condensation of a chondritic vaporized impactor inside a vapor impact plume.

These types of Mössbauer measurements have also been carried out by Verma et al. (2001) and Bhandari et al. (2002), who identified the same distinct superparamagnetic phase with sizes varying between a few nanometers (K-T boundary layer at Anjar, Meghalaya, and Turkmenistan sections) and

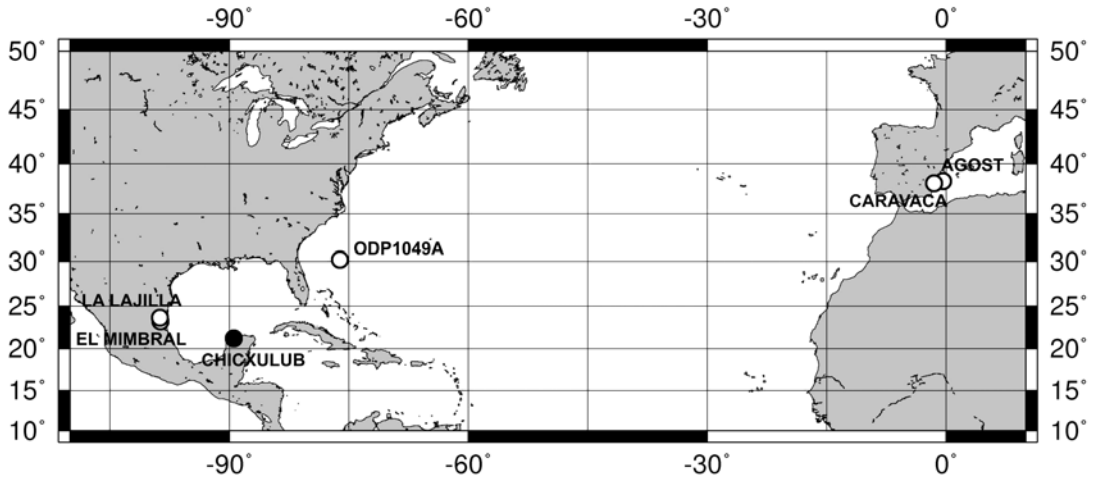

Fig. 1. Geographic location of investigated sections (white circles) and Chicxulub impact structure (black circle).

tens of nanometers (Gubbio). This nanophase is reported to be made of iron oxides/oxyhydroxides like hematite and goethite. These authors support a meteoritic origin of this Fe-nanophase in the form of iron nanoparticles condensed from the impact vapor cloud, deposited globally and subsequently weathered to oxides/oxyhydroxides. Verma et al. (2001) also measured some samples from a ferruginous layer at the Permian-Triassic boundary in the Attargoo section (India) and found a similar nanophase, although no iridium anomaly was detected and therefore no clear association with an impact event can be drawn. Mössbauer analysis of Verma et al. (2001), Bhandari et al. (2002), and Wdowiak et al. (2001) did not detect any signal of the Mg- and Ni-rich spinels that are known to be present at the K-T boundary. They also did not detect any Mössbauer feature due to magnetite as the magnetite reported by Worm and Banerjee (1987) and Griscom et al. (1999).

Another type of study was performed by Ten Kate and Sprenger (1993), who used bulk magnetic susceptibility as a proxy for $CaCO_3$ content in marine sediments in the Zumaia section (northern Spain). They detected an increase in susceptibility in the K-T boundary clay layer, but they did not discuss its significance. D'Hondt et al. (1996) used continuous magnetic susceptibility measurements to study climatic cyclicity in four DSDP K-T boundary sections in the southern Atlantic Ocean, reporting also an increase in magnetic susceptibility associated with the K-T boundary clay layer, but did not discuss it further.

With these varied but somehow fragmentary and sometimes contradictory precedents, our study intends to properly characterize the magnetic properties of K-T boundary sediments in a variety of proximal and distal sections in order to achieve useful information concerning quite different aspects of the problem: does a coherent magnetic signature of the K-T boundary layer exist? Is this signature related to the extraterrestrial material input? Could rock magnetic properties tell us anything about the type of material emplaced by the impact in a globally distributed ejecta layer and about the geographical patterns of this emplacement? Some interesting information has been obtained pertaining to all these subjects, but further work needs to be developed in all the mentioned areas. This K-T boundary investigation can be connected to a broader scope: the possibility that macroscopic rock magnetic properties can serve as a useful tool in order to locate and identify stratigraphic layers associated with major meteoritic impacts occurred at different geological times.

DESCRIPTION OF THE INVESTIGATED SECTIONS

Several distal and proximal sections have been investigated in the Northern Hemisphere (Fig. 1). The most distal sections were sampled in the Iberian Peninsula at Agost and Caravaca. At the time of the Chicxulub impact event, they were approximately 7000 km away from the impact crater. At a lesser distance, ~1700 km to the northeast of Chicxulub, on the North American margin, the K-T boundary interval was also investigated at ODP Leg 171B Hole 1049A (Blake Nose Plateau, near the Florida-Georgia shoreline). Regarding proximal sections, samples have been taken from El Mimbral and La Lajilla, situated in northeastern Mexico about 1000 km away from Chicxulub crater.

Agost and Caravaca

Agost and Caravaca sections belong to the External Zones of the Betic Cordillera (southeast Spain), and can be considered to be twin sections, although Caravaca was originated in a somewhat deeper sedimentary environment, and certain differences occur in the diagenetic history experienced by the very thin red clay layer that defines the K-T boundary (Martínez-Ruiz et al. 1999). Both sections

developed in a pelagic environment, and the sediment deposition during the late Maastrichtian and the early Danian resulted in sequences of marls and marly limestones. The K-T boundary is marked in both sections by a reddish clay layer ~2 mm thick that represents the meteoritic-rich dust dispersed and deposited globally after the impact event. Above this thin layer, a greenish to grayish clay layer ~5 to 15 cm thick was deposited as a result of the sudden decrease in ocean productivity. Its carbonate content gradually increases, giving way to the Danian marly lithologies. Within the ~2 mm thick K-T layer (hereinafter the fireball layer), several impact markers have been found: iridium spike and other geochemical anomalies (Smit and Hertogen 1980; Smit and Ten Kate 1982; Martínez-Ruiz et al. 1992; Martínez-Ruiz 1994); shocked quartz grains (Bohor et al. 1987); Mg- and Ni-rich spinels (Bohor et al. 1986; Robin et al. 1991); and microspherules considered to be diagenetically altered microkrystites (Smit and Klaver 1981; Martínez-Ruiz 1994; Martínez-Ruiz et al. 1997). These microspherules, with mean sizes between 100 and 500 microns, are composed of iron-oxide (Fe-O spherules) or K-feldspar, and their relative abundance establishes a difference between the two sections. Iron oxide spherules are mainly recovered from Agost section and are absent in Caravaca, where some iron oxide particulates occur but with no spherical shapes and in low quantities, mostly corresponding to altered pyrite framboids. K-feldspar spherules are recovered from both sections (Smit and Klaver 1981; Martínez-Ruiz 1994; Martínez-Ruiz et al. 1997). In some K-feldspar spherules, inner carbon-rich cores of mafic compositions are detected and interpreted as a relict of the original material composing the microkrystites (Martínez-Ruiz 1994; Martínez-Ruiz et al. 1997).

Blake Nose, ODP Hole 1049A

During Leg 171B, the Ocean Drilling Program recovered a K-T boundary interval at different holes drilled on the North American margin in the Blake Nose Plateau. A spherule bed 9 to 17 cm thick occurred at the biostratigraphic boundary between the Cretaceous and the Paleocene at Site 1049. The spherule bed sharply overlies slumped uppermost Cretaceous foraminiferal-nanofossil ooze and is overlain by Tertiary clay-rich ooze. For this study, we have studied samples from Hole 1049A (1049A-17X-2), in which the K-T boundary layer presents the largest thickness. This bed also contains some lithic fragments, Cretaceous foraminifera, and clasts of Cretaceous material, which indicate reworking and downslope transportation of the spherule bed material (Klaus et al. 2000). At Hole 1049A, the K-T boundary is marked by a bed 17 cm thick that is mostly composed of green spherules, with spherical and oval shapes ranging in size between 100 and 1000 microns. These spherules derived from impact-glass-generated material and diagenetically altered to smectite (Martínez-Ruiz et al. 2001a). Such impact glass, on the basis of the available evidence, is thought to have been generated from Si-rich and Ca-rich target material. At the very top of the spherule bed, there is an orange limonitic layer 3 mm thick. Originally, it was interpreted as the fireball layer, similar to the upper red layer found in North America western interior sections (Norris et al. 1998). But more recently, Martínez-Ruiz et al. (2001b) indicated that the geochemical composition of this limonitic layer is similar to the rest of the spherule bed except for an enrichment in iron. This, together with the fact that the iridium spike detected in this section was not coincident with the limonitic layer, but instead with the first centimeters of Tertiary ooze, led Martínez-Ruiz et al. (2001b) to suggest that the limonitic layer is related to a diagenetic remobilization of iron.

El Mimbral and La Lajilla

At the El Mimbral section, the Maastrichtian and the Danian are represented by hemipelagic marls of the Mendez (Cretaceous) and Velasco (Paleogene) formations, deposited at depths of over at least 1000 m (Alegret et al. 2001). Between them, a complex channelized siliciclastic deposit up to 3 m in thickness is observed. This siliciclastic pack is divided into roughly two parts. The basal part is a coarse and poorly graded spherulitic bed up to 1 m thick, composed of spherules mostly altered to calcite or chlorite-smectite, although some glass cores have been reported to occur (Smit et al. 1992), with compositions relating them to Chicxulub target ejecta. The second part of the siliciclastic complex consists of several sandstone beds that have been subdivided in different ways according to sedimentary structures and grain size. Smit et al. (1992, 1996) divided it in two separate units: the lower one (unit 2) corresponds to massive parallel laminated calcarenite beds (described instead as quartzose sandstone cemented by calcite by Bohor 1996); the upper one (unit 3) is about 20 cm thick and consists of several rippled layers of fine calcareous sandstone, intercalated with finely laminated silttites and mudstones. A different subdivision has been made by Bohor (1996), who identified the succession of sandstone beds as a turbidite Bouma sequence (T_a–T_e). On top of the sandstone complex and gradually giving way to the first Velasco hemipelagic marls, there is a clay-rich interval 4 cm thick. In the edges of the channelized deposit, an orange-red layer several mm thick is embedded within this clay-rich interval. This reddish layer has been reported by several authors: Keller et al. (1994) called the clay-rich interval the “K-T boundary clay” and placed the K-T boundary at the reddish layer; Smit et al. (1996) included this interval in the uppermost part of their unit 3, and described the reddish layer as a flaser-like fine-sandstone layer cemented by goethite and not corresponding to the so-called fireball layer of distal K-T sections; Bohor (1996) interpreted this clay-rich interval as the low-energy fallout corresponding to the T_e Bouma division; finally, this layer is, presumably, the one that

Wdowiak et al. (2001) subjected to Mössbauer analysis, assuming it was similar to the fireball layer of the North America western interior sections. Regarding Ir abundances, Smit et al. (1996) reported small enrichments in the silt rippled layers of their unit 3, and a maximum of ~0.9 ppb in the reddish-goethite layer. Stinnesbeck et al. (1993) reported maximum abundance of 0.8 ppb in the clay-rich interval on top of the sandstones. López-Oliva and Keller (1996) and Keller et al. (1997) reported Ir abundances across the upper part of the siliciclastic pack, obtained in the far western edge of the channel. According to them, Ir abundances inside the clay-rich layer were between 0.3 and 0.5 ppb, higher than the 0.2 ppb detected in the uppermost sandstones but lower than the maximum of 0.8 ppb detected in the lowermost Velasco marls. Rochia et al. (1996) studied both Ir and Ni-rich spinels and reported relative enrichments of both in the finest rippled layers of Smit's unit 3, a maximum Ir concentration of 0.5 ppb on top of this unit and a maximum of 300 Ni-rich spinels per gram some centimeters below the Ir maximum. In order to construct a composite section including all the relevant lithologies, we have taken samples from the main body of the siliciclastic outcrop (Mendez marls, spherule bed, lower and middle sandstones; next to the 30 m red mark painted by Smit et al. 1992) and from the western edge of the deposit around 30–40 meters apart from the first point (upper sandstones, clay-rich layer, and Velasco marls).

La Lajilla section is 50 km to the northwest of El Mimbral and can be regarded as a compressed version of the latter. Again we find Mendez and Velasco marly formations, separated by a siliciclastic body that has been subdivided as El Mimbral. The main difference between El Mimbral and La Lajilla is the thickness of the siliciclastic strata. In La Lajilla, the spherule bed is 20–25 cm thick, whereas the sandstone beds sum up to 100–105 cm. In La Lajilla, the contacts between the spherule bed and Mendez marls and sandstones are marked by the presence of altered reddish material, sharply defined at the lower contact (although somehow irregular), and more diffuse and spread at the upper transition. Additional footprints of post-depositional alteration can be seen as irregularly distributed reddish material embedded within the spherule bed. The sandstone pack is followed by a silt-clay-rich layer 4 cm thick and enriched in Ir (Smit et al. 1996; Bohor 1996). The Velasco marls above this layer also have high Ir concentrations. No reddish layer is observed within this clay-rich interval. Bohor (1996) reported Ni-rich spinels in low numbers in this clay-rich layer. In this case, we have also sampled the lower and upper lithologies in two places at opposite sides of the creek, some meters apart, to construct a composite section.

Regarding the significance and dating of the siliciclastic deposit, most authors (Smit et al. 1992, 1996; Bohor 1996; Rochia et al. 1996; Bralower et al. 1998; Soria et al. 2001; Arz et al. 2001; Alegret et al. 2002; Lawton et al. 2005) consider that the normal end-Maastrichtian hemipelagic sedimentation was interrupted by the Chicxulub impact, which emplaced target ejecta in the form of glassy spherules and shocked quartz in sedimentary basins around the Gulf of Mexico. These ejecta, partially or totally altered by diagenesis and mixed up with some upper Cretaceous eroded material, would account for the spherule layer. After the emplacement of the ejecta, sand and debris were removed from shallower environments and deposited over the spherule bed, either by the megatsunamis that have been proposed to have followed the impact (Smit et al. 1992, 1996) or by impact-triggered sediment gravity flows around the Gulf of Mexico (Bohor 1996; Bralower et al. 1998; Soria et al. 2001; Arz et al. 2001; Alegret et al. 2002). The silt and clay-rich layers on the top part of the sequence would correspond to the deposition of the finer fraction of these abnormally reworked siliciclastic sediments in a progressively less energetic sedimentary environment. These fine sediments would have settled with the finest fraction of the impact-generated material, and therefore would appear enriched in the extraterrestrial components.

METHODOLOGY

After sampling the reported sections at different resolutions depending on outcrop conditions, rock magnetic measurements were performed in the Paleomagnetism Laboratory of the Complutense University of Madrid (Spain), and additional experiments were carried out in the Palaeomagnetism Laboratory of ETH Zürich (Switzerland). Magnetic susceptibility was measured with a Kappabridge KLY-3 (Agico); each sample was measured at least ten times and averaged. Isothermal remanent magnetization (IRM) acquisition curves have been imparted with an impulse magnetizer (ASC Scientific IM-10-30) and measured with either a spinner magnetometer JR-5A (Agico) or a 2G SQUID magnetometer. Maximum peak fields were above 2 T. Hysteresis and remanence cycles up to 0.5 T were measured with the Coercivity Spectrometer developed by Kazan University (Burov et al. 1986) and sited at Madrid Paleomagnetism Laboratory; each data point was measured 9 times and averaged; magnetic field increments of 0.5 mT were used. Demagnetization of a three-axis composite IRM was performed with a Schondsted furnace and a JR-5A spinner magnetometer. Thermomagnetic curves were acquired with the horizontal Curie balance of Zürich Laboratory (bulk samples, operation field 1 T) and with the instrumentation at Kazan University (separate of iron oxide spherules, operation field 0.2 T).

In Figs. 2, 10, 12, and 13, three different magnetic parameters are plotted for each section. The first one, bulk magnetic susceptibility, is affected by all the minerals present in a sample, but it is dominated by the ferromagnetic fraction if it is present in enough quantities. The second parameter, saturation isothermal remanent magnetization (SIRM), is the

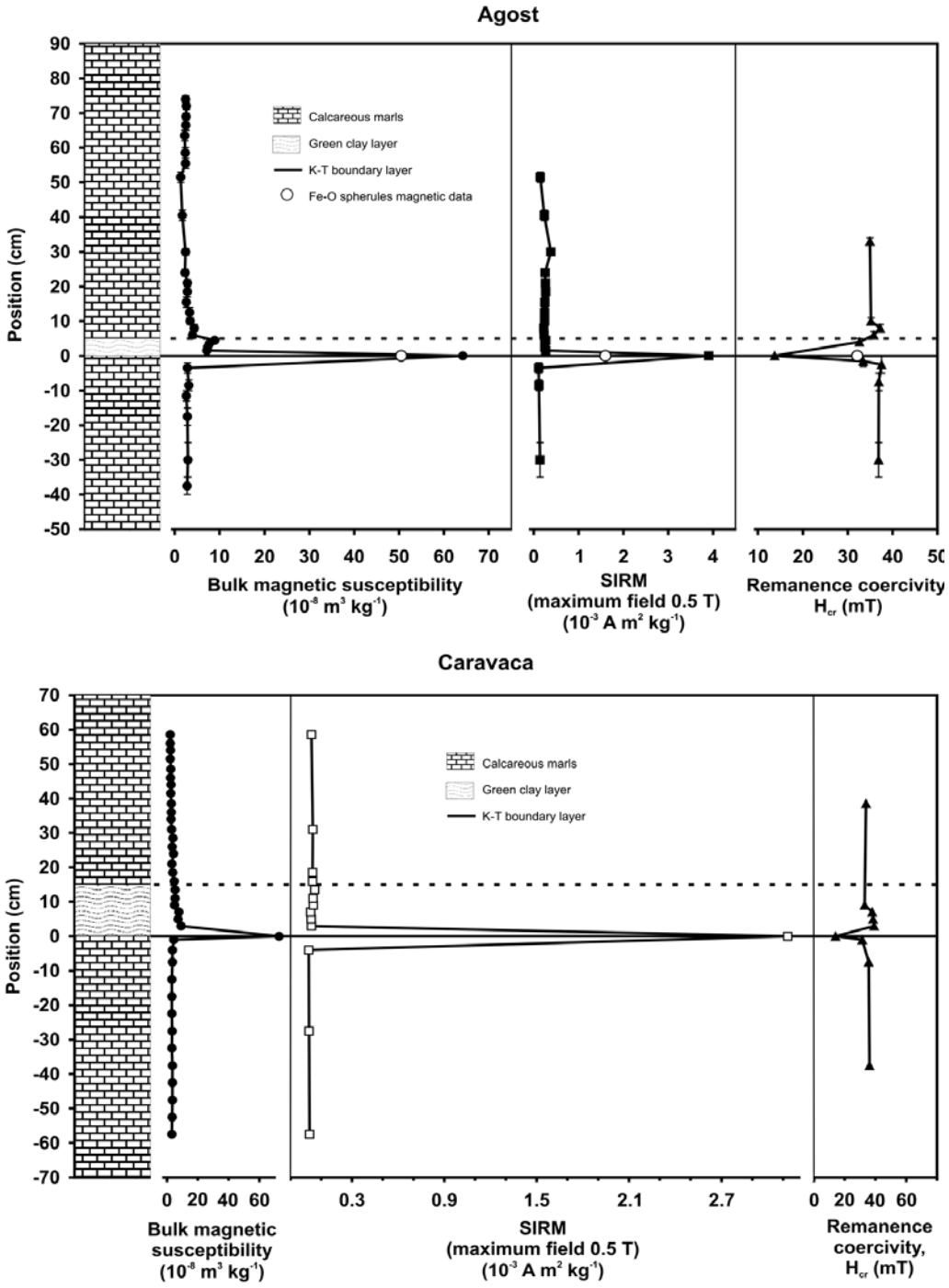

Fig. 2. Magnetic properties across K-T boundary at Agost (top) and Caravaca (bottom).

remanent magnetization acquired by the sample under the maximum magnetic field applied during the measurement of the remanence curve. This parameter depends both on the proportion of ferromagnetic material in the sample and on the mineralogical nature of this ferromagnetic fraction. For qualitative comparison, pure magnetite and similar ferrimagnetic phases (like maghemite or magnesioferrites) have saturation magnetizations up to two orders of magnitude higher than hematite or goethite. The third parameter is remanence coercivity (H_{cr}), corresponding to the magnetizing field that needs to be applied to a sample previously saturated in the opposite direction in order to eliminate its remanent magnetization. It strongly depends on the mineralogical nature of the magnetic phases present in the sample.

Ferrimagnetic minerals like magnetite, maghemite, and magnesioferrites have low-remanence coercivities; iron sulfides have intermediate values; hematite has significantly higher values; and goethite has even higher remanence coercivities. Usually, low remanence coercivity minerals are called "soft" magnetic minerals, while high remanence coercivity minerals are referred to as "hard" magnetic minerals. Magnetic parameters also depend on the magnetic state of the ferromagnetic fraction (i.e. single-, pseudosingle- or multidomain), but the previous sentences can serve as a first guide to the meaning of the behavior of the three plotted magnetic parameters. For a proper and lengthy discussion about rock magnetism and the significance of each magnetic parameter and experiment, see, for example, Dunlop and Özdemir (1997).

As trace and major element data were not available in the literature, additional geochemical analyses were carried out on samples from El Mimbral. Concentration of typical extraterrestrial elements was used as evidence of the contribution of the meteorite derived material. Trace and major element analyses were performed by inductively coupled plasma mass spectrometry (ICP-MS) and atomic absorption spectrometry (AAS) respectively after sample digestion with HNO_3 + HF, and using a Perkin Elmer Sciex Elan-500 and a Perkin Elmer 5100 spectrometer from the Analytical Facilities of the University of Granada (Spain). The precision expressed as relative standard deviation for different major elements ranges from 0.2% to 2%. For trace elements, precision was better than ±2% and ±5% rel. for analyte concentrations of 50 and 5 ppm, respectively. Bulk mineral composition of Agost iron oxide spherules was also determined by X-ray diffraction with a Siemens Kristalloflex 810 diffractometer.

Due to the various and contradictory iridium abundance profiles published for El Mimbral, iridium and other PGE abundances were measured in 11 samples from this section covering all the relevant lithologies and focussing specially in the transition between sandstones, clay-rich layer, and Velasco marls. Nickel sulphide fire assay with ICP-MS finish was used. The measurements were performed by Geoscience Laboratories (GeoLabs, Sudbury, Canada). Instrumental detection limits in ppb were: Ru 0.13; Ir 0.04; Pd 0.11; Pt 0.14; Au 0.71.

MAGNETIC PROPERTIES AT AGOST AND CARAVACA SECTIONS

Bulk magnetic susceptibility, maximum value of isothermal remanent magnetization (SIRM), and remanence coercivity (H_{cr}) for Agost section are shown in Fig. 2 (top). An iron oxide (Fe-O) spherule separate from the fireball layer was also analyzed and is represented in Fig. 2 as white circles. The spherules were hand-picked one by one from the bulk sample with the aid of a binocular lens. As can be seen, the fireball layer is associated with a sharp increase in susceptibility and SIRM, indicating much higher abundance of ferromagnetic minerals. The corresponding decrease in remanence coercivity indicates that the magnetic phase responsible of this magnetic spike is much softer (magnetically) than the magnetic phases present in under- and overlaying materials. The behavior of the Fe-O spherules is clearly different from the bulk fireball layer sample, with lower mass susceptibility and SIRM and higher remanence coercivity, similar to the values observed in Cretaceous and Tertiary materials. This means that the magnetic phase responsible of the peculiar characteristics of the fireball layer is not completely contained within the spherules. This result is in strong contrast with Worm and Banerjee (1987) and Cisowski (1988).

Results for Caravaca section are displayed in Fig. 2 (bottom). The pattern is quite similar to that of Agost, with increases in susceptibility and SIRM values at the fireball layer and a similar decrease in remanence coercivity. In this case, Fe-O spherules were not present, and therefore no extraction was performed. Again, we find a distinct magnetic phase present only in the fireball layer and not concentrated in any Fe-O spherules.

Clearly, the magnetic spike associated with the fireball layer is not only a result of higher concentration of ferromagnetic materials, but also of a difference in magnetic mineralogy. First, it is possible to ask if these increases in susceptibility and SIRM are just apparent, since the K-T boundary layer corresponds to a sharp decrease in carbonate content and hence to an increase in ferruginous fraction. Since the magnetic parameters are normalized by mass, this would appear as an increase in susceptibility and SIRM values, even without any changes in the magnetic mineralogy or in the concentration of ferromagnetic material within the ferruginous fraction. To discard this possibility, a correction of the magnetic susceptibility values by the carbonate fraction has been performed and the results are shown in Fig. 3. To perform this correction, data on calcite percentage in bulk samples has been taken from Martínez-Ruiz (1994). The carbonate fraction drop can explain the slightly higher susceptibility values of the boundary dark clay in Agost, but not the fireball layer magnetic spike. Moreover, remanence coercivity by itself indicates differences in magnetic phases and not just in concentration. Additionally, looking at the IRM acquisition curves (Fig. 4), it can be observed that the coercivity spectrum of the fireball layer sample is clearly displaced toward lower magnetic fields when it is compared with under and overlaying samples.

The IRM acquisition curves of the fireball layer, especially in Agost, show a small contribution from a high coercivity phase (saturation not reached at 2–2.5 T). This phase could correspond to goethite, probably the one detected by Wdowiak et al. (2001). Goethite saturation magnetization is two orders of magnitude lower than that of magnetite and

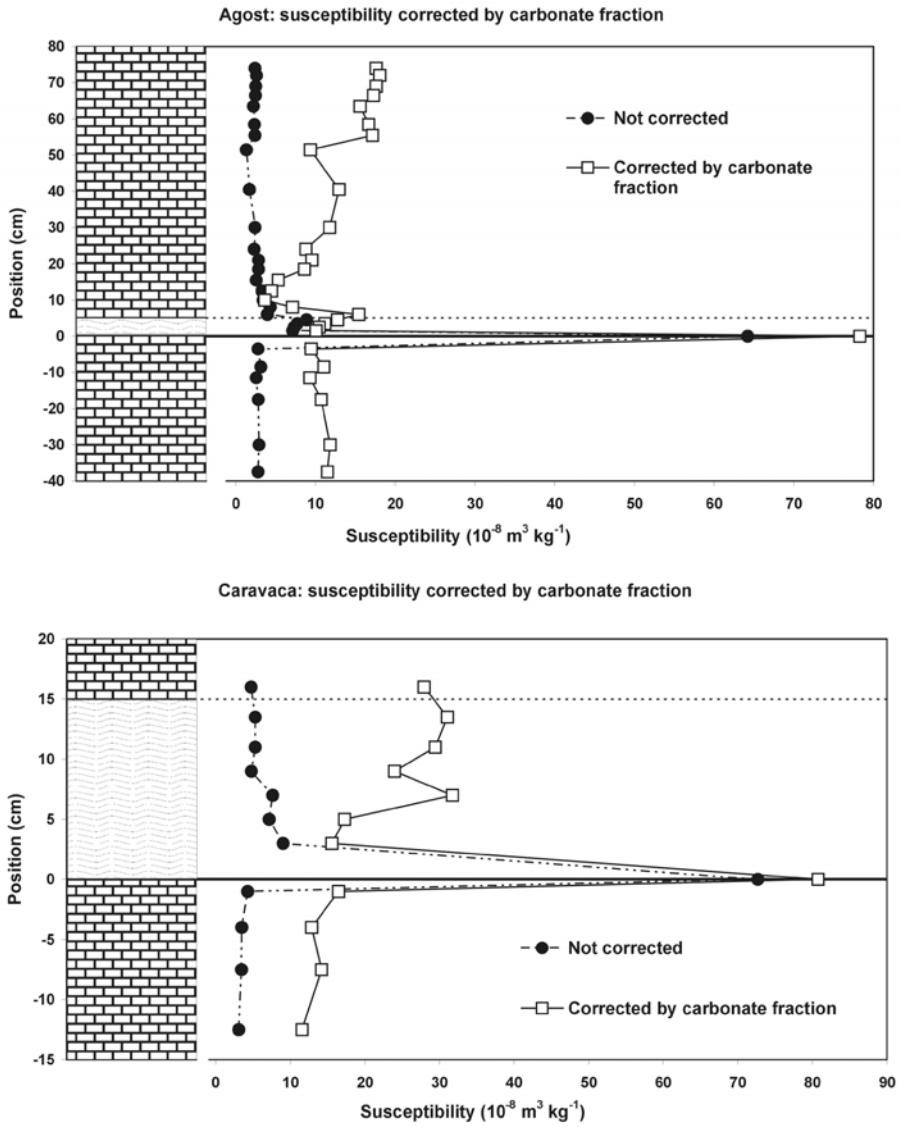

Fig. 3. Susceptibility corrected by carbonate fraction for Agost and Caravaca.

similar ferrimagnetic phases, and thus its relative abundance must be high in order to be appreciable in the IRM curves, which are controlled by the much more intense low coercivity phase. This would explain why the Mössbauer analysis detect the goethite contribution but are insensitive to the less abundant low-coercivity phase, while the rock magnetic properties are controlled by the latter.

Thermomagnetic measurements for two bulk samples from Agost K-T fireball layer are shown in Fig. 5a. In both samples we see a steeped decrease in saturation magnetization around 100–110 °C, possibly due to the presence of goethite. A second decrease is observed between 300 and 350 °C. In sample 1, another decrease is observed around 650 °C, indicating the presence of some hematite, but this is not duplicated in sample 2. Another important feature of both samples is the irreversible character of the curves. The cooling branches are different from the heating ones, and the magnetic phase responsible for the decreases between 300 and 350 °C in the heating curves is destroyed by heating, and a new phase with lower saturation magnetization is created, at least in sample 1, where it can be identified as hematite.

Thermomagnetic measurements were also performed on the Agost Fe-O spherules extraction (Fig. 5d). Temperature instabilities during cooling prevented the measurement of the cooling branch of the curve; a second heating curve was therefore measured. As in the bulk samples, a steeped decrease is observed between 250 and 350 °C, and the curve is again irreversible, with the phase responsible of this main decrease destroyed by heating. The second curve indicates that magnetic phases with lower magnetization are present after heating. Increases in magnetization are observed in both curves at high temperatures, possibly corresponding to

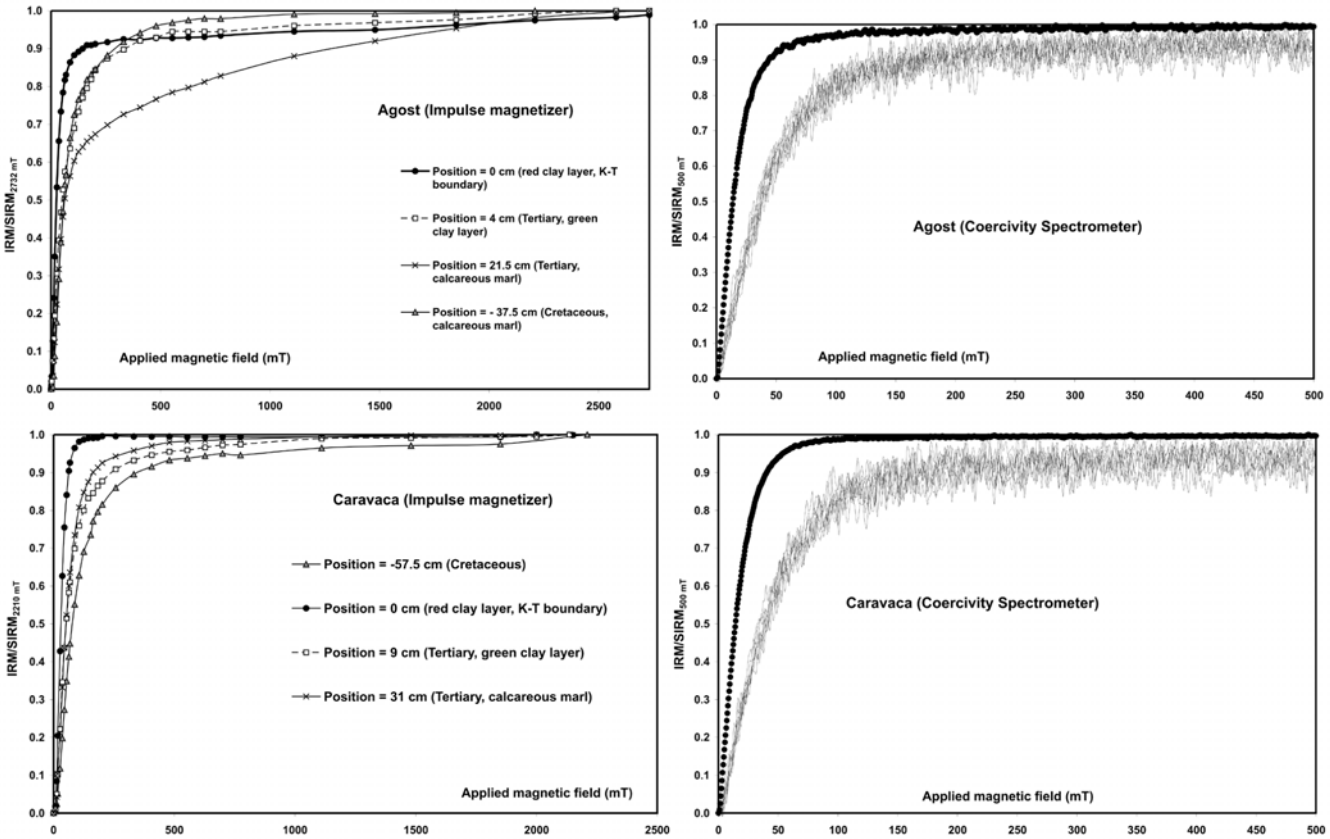

Fig. 4. IRM acquisition curves for Agost (top) and Caravaca (bottom) samples. Left: IRM imparted with an impulse magnetizer up to 2.5 T to selected samples. Right: IRM imparted and measured with a coercivity spectrometer. Black solid circles correspond to fireball layer; thin lines correspond to the rest of lithologies.

chemical changes and thermal activation effects near the Curie temperature. In the first curve, the peak is centred on 575 °C, revealing a magnetite-like behavior. In the second curve the peak is placed at higher temperatures, around 615 °C, indicating that after destroying the main magnetic phase, a tendency toward hematite-like behavior is developed. Despite the different nature of the measurements performed on bulk samples (1 T field) and spherules (200 mT field), a similar behavior is observed in both cases. In summary, in the Agost fireball layer (bulk sample), the main magnetic phase has irreversible transformation temperatures around 300–350 °C. This phase is destroyed by heating. Some traces of goethite and hematite can also be observed, at least in one sample, and some hematite is created by heating in one sample, possibly as a result of goethite dehydration. A very similar behavior is observed in the iron oxide spherules, and thus the differences in magnetic composition between bulk sample and spherules, revealed by differences in remanence coercivities, are not apparent in thermomagnetic measurements.

The differences in magnetic mineralogy between bulk sample and Fe-O spherules are evident when the IRM acquisition and back-demagnetization curves for Fe-O spherules are plotted. In Fig. 6, we see that the Fe-O spherules IRM acquisition is dominated by two main phases, one with low coercivity (saturation fields below 100 mT) and the other with high coercivity (saturation and maximum gradient are not reached). In addition, when the applied magnetic field begins to decrease from 0.5 T to zero, the acquired IRM begins to experience a rather apparent relaxation with a linear trend. This informs us that an important fraction of the magnetic carriers is in superparamagnetic state (providing that the total time elapsed between H = 0.5 T and H = 0 T is 600 s or 10 min), and therefore fine grain sizes are expected. The low-coercivity phase revealed in IRM acquisition is with high probability the one responsible for the decrease of magnetization observed in thermomagnetic curves between 250 and 350 °C. Since no clear signal of hematite is shown in the thermomagnetic first heating curve, the characteristics of the high-coercivity phase lead to identify it as fine-grained goethite. This is supported by X-ray diffraction patterns (Fig. 7).

Thermal demagnetization of an IRM imparted along three orthogonal axes (Lowrie 1990) has been performed in order to further constrain the coercivities and unblocking/ chemical transformation temperatures of the magnetic phases

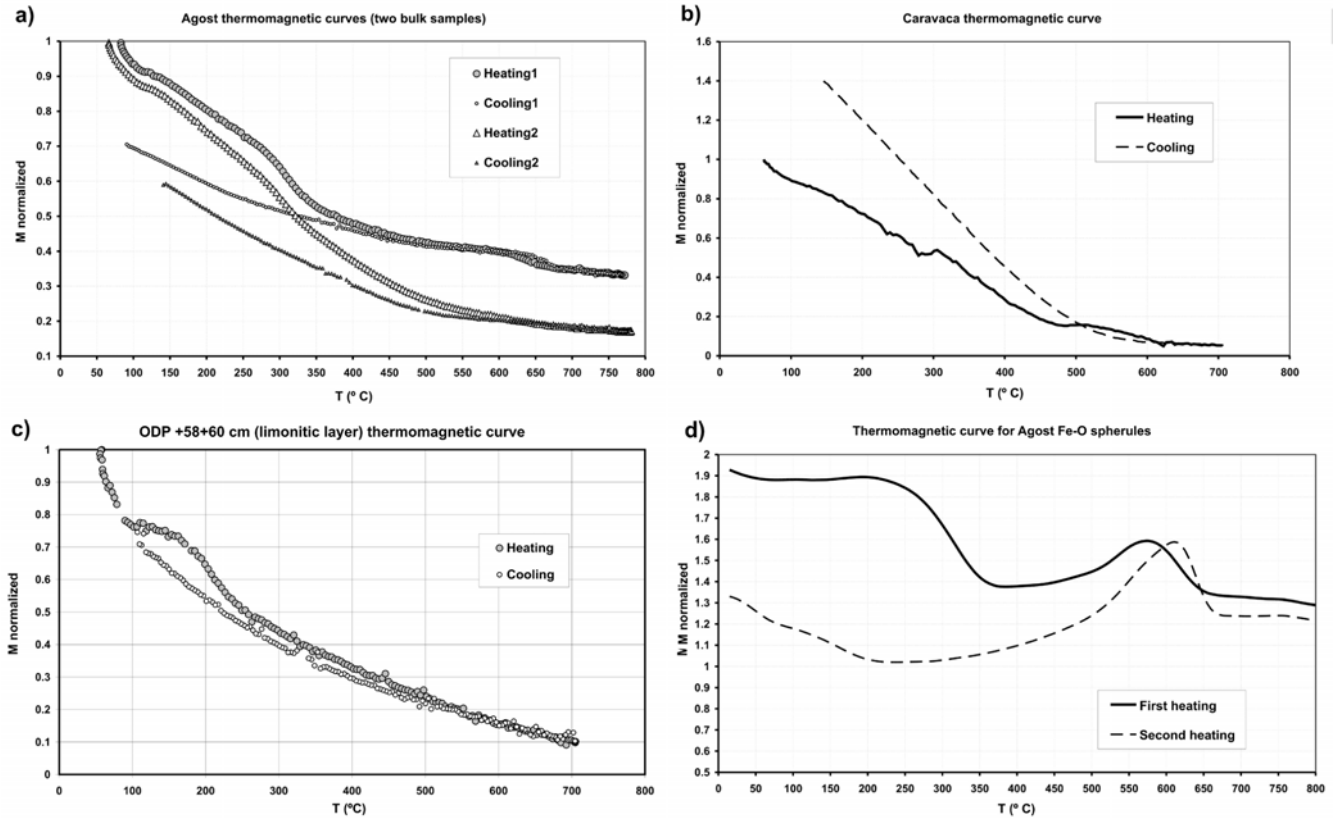

Fig 5. Thermomagnetic curves for (a) Agost fireball layer bulk samples; (b) Caravaca fireball layer bulk sample; (c) ODP Hole 1049A limonitic layer bulk sample; (d) and Agost Fe-O spherules extraction. Curves (a), (b), and (c) were measured in a magnetic field of 1 T, while (d) was measured with a different instrument in a 0.2 T magnetic field.

present in the samples. In Fig. 8 (top), results for the Agost fireball layer (bulk sample) are shown. Most of the IRM is concentrated in the soft axis with coercivities below 0.12 T, and it falls in a gradual trend to almost zero below 450 °C, with perhaps partial fallings around 120 and 300 °C. A small but still appreciable fraction of the total magnetization is present in the hard axis, with coercivities between 0.4 and 2 T. The magnetization in this axis is more or less constant until its sudden drop around 650 °C, identifying it as hematite. A partial fall, not clearly seen in our data, could be present in the hard axis below 100 °C, indicating the presence of goethite. No significant fraction of the IRM is contained in the 0.4 T axis, its noisy character being due to sample orientation errors during measurements, that cause partial projections of the IRM attained in the other axes, mainly the most intense one, onto the 0.4 T axis.

Thermomagnetic curves for Caravaca fireball layer are plotted in Fig. 5b. The data are of poorer quality, but the main features can still be addressed. A smooth decrease in saturation magnetization is observed up to 450 °C, with perhaps a previous partial fall around 275 °C. One more fall of magnetization is present around 600 °C. The curve is again irreversible, and the magnetic phases responsible for these decreases are destroyed by heating. In contrast to the Agost results, the Caravaca cooling curve shows higher values of magnetization than the heating curve below 500 °C. As in the case of Agost, the irreversibility of the curves prevents us from univocally identifying any Curie point, but some important information has been gained.

Thermal demagnetization of an IRM imparted along three orthogonal axes has also been carried out in Caravaca fireball layer (Fig. 8, bottom). Apart from the higher intensities in Caravaca sample, the behavior is quite similar to that observed in the Agost bulk sample, with most of the IRM concentrated in the soft axis and decaying gradually before 450 °C. Partial drops are suggested around 115 and 300 °C, as before. In the case of Caravaca, no significant magnetization is measured in the other two axes, and therefore no hematite is detected. The presence of some hematite in Agost and its absence in Caravaca deduced from IRM demagnetization experiments is coherent with thermomagnetic measurements.

The thermomagnetic and IRM demagnetization results are clearly different from those of Worm and Banerjee (1987), who found magnetite as the main magnetic phase in Petriccio magnetic spherules. No similar result is reached in Agost and Caravaca, either in bulk samples or in Fe-O spherules. Agost and Caravaca thermomagnetic behavior is similar to that reported by Cisowski (1988) for Petriccio.

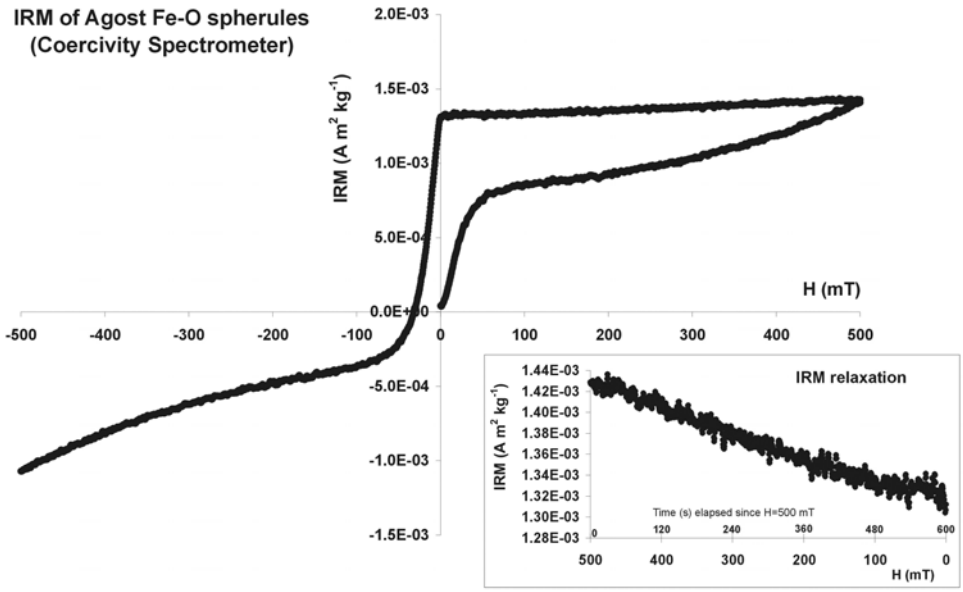

Fig. 6. IRM acquisition and back-demagnetization curves for Agost Fe-O spherules. Inset: IRM relaxation between maximum (0.5 T) and zero applied magnetic fields.

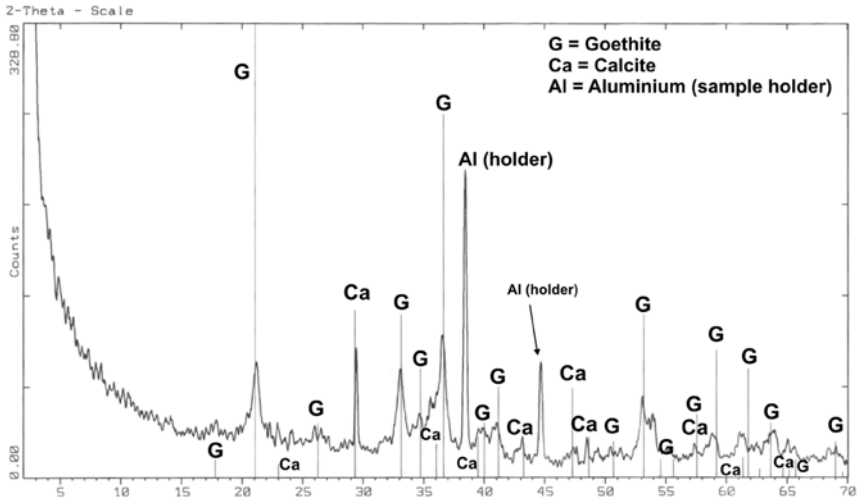

Fig. 7. X-ray diffraction pattern for Agost Fe-O spherules with superimposed goethite, calcite, and aluminum (holder) lines.

The fact that no significant goethite signal is detected in this IRM demagnetization data, though it is clearly present in Agost Fe-O spherules, could be explained by the high thermal relaxation of this phase.

Finally, magnetic properties at low temperatures have been investigated in fireball layer bulk samples, both in Agost and Caravaca, and also in the Fe-O spherules separate from Agost. Zero field heating up to room temperature of an SIRM acquired at 5 K (maximum field of 9 T) was measured (Fig. 9). The main feature is that no Verwey transition is observed in any of the samples (compare with the curve for a magnetite-bearing peridotite in Fig. 9). This lack of Verwey transition, along with the ample evidence provided by the other experiments, implies that no pure magnetite is detected in our samples, which is in contrast to the findings of Worm and Banerjee (1987). To explain the observed magnetic characteristics of the fireball layer magnetic spike (high susceptibility and SIRM, low-remanence coercivities, transformation/unblocking temperatures between 300 and 450 °C) we have to appeal to another mineral. As we will see in the discussion, the main candidate is magnetite-like spinel with significant cation substitution and high oxidation states (oxidation of magnetite, i.e., maghemitization, is a well-known mechanism to suppress the Verwey transition) (Dunlop and Özdemir 1997).

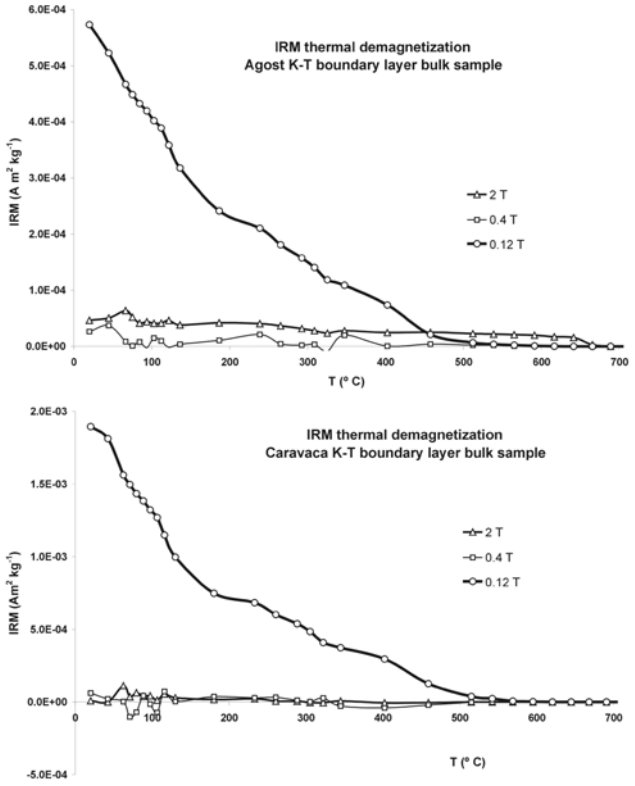

Fig. 8. Thermal demagnetization of an IRM imparted along three orthogonal axes for Agost (top) and Caravaca (bottom) fireball layer bulk samples.

MAGNETIC PROPERTIES AT BLAKE NOSE SECTION

In Fig. 10 (top), bulk magnetic susceptibility, SIRM, and remanence coercivity profiles are shown for the ODP Hole 1049A K-T boundary interval. In the susceptibility profile, sample at 58–60 cm depth in section (1049A-17X-2) includes the limonitic layer described above. Susceptibility is plotted both for bulk sample and for limonitic material alone (gray rhombus); the curves for the other two parameters included at this position values just for the limonitic material. For comparison, Fig. 10 (bottom) shows the susceptibility profile (ODP+58+60 cm bulk sample) measured in this work along with the susceptibility data reported by the ODP scientific shipboard party (Norris et al. 1998). Normalization by the highest value of each curve was performed for comparison purposes, since the on-board measurements were made with a continuous core susceptibility meter and hence no mass normalization is possible; our measurements are discrete and mass-normalized. The general pattern coincides, and differences could be due to different types of measurements: on-board data points include contribution from surrounding material while discrete measurements do not; on the other hand, discrete measurements do not average contribution for all the material at the same core depth, while continuous measurements do. What is clearly seen is that the limonitic

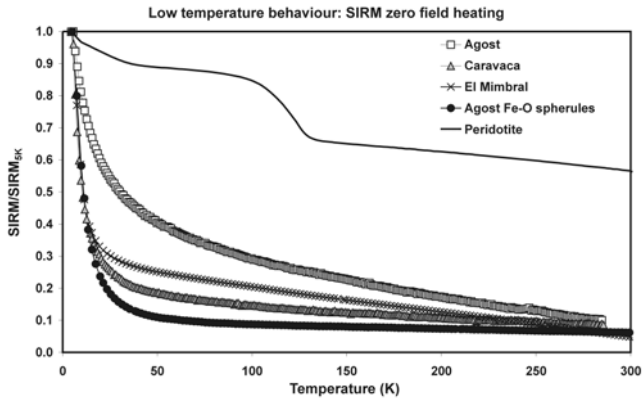

Fig. 9. Zero field heating of SIRM acquired at 5 K and 9 T for Agost and Caravaca fireball layer bulk samples, Agost Fe-O spherules extraction, El Mimbral reddish layer and a magnetite-bearing peridotite for comparison.

layer presents a sharp anomaly with very high values of susceptibility, SIRM, and remanence coercivity. This anomaly is not seen in the continuous log, since it is masked by the surrounding material signal.

The magnetic phase responsible of the anomaly in the limonitic layer is very different in nature from that reported in Agost and Caravaca, where remanence coercivities lower than those of surrounding material were found. At Blake Nose, the remanence coercivity of the limonitic layer is extremely high. Figure 11 shows the IRM acquisition and back-demagnetization curves for this layer and the underlaying and overlaying material. As we can see, although there is a contribution from a low-coercivity phase, the magnetic behavior of the limonitic layer is strongly controlled by a high-coercivity phase, and the IRM acquired by this phase presents a significant relaxation with time. This is similar to the high-coercivity phase that was observed in Agost Fe-O spherules, and it is indicative of the presence of goethite with fine grain sizes.

Figure 5c shows the thermomagnetic behavior of the ODP sample including the limonitic layer. A step decrease at low temperatures is compatible with goethite presence, and a small ferromagnetic fraction is revealed with transformation temperatures between 200 and 230 °C. This phase is totally destroyed by heating and is absent from the cooling branch, and with high probability corresponds to the low coercivity phase contribution revealed in the IRM curves.

MAGNETIC PROPERTIES AND GEOCHEMICAL COMPOSITION AT EL MIMBRAL AND LA LAJILLA SECTIONS

Magnetic Properties

As can be seen in Figs. 12 and 13, the magnetic behavior in El Mimbral and La Lajilla is more complex than in the distal sections. In the El Mimbral profile, a spike in magnetic

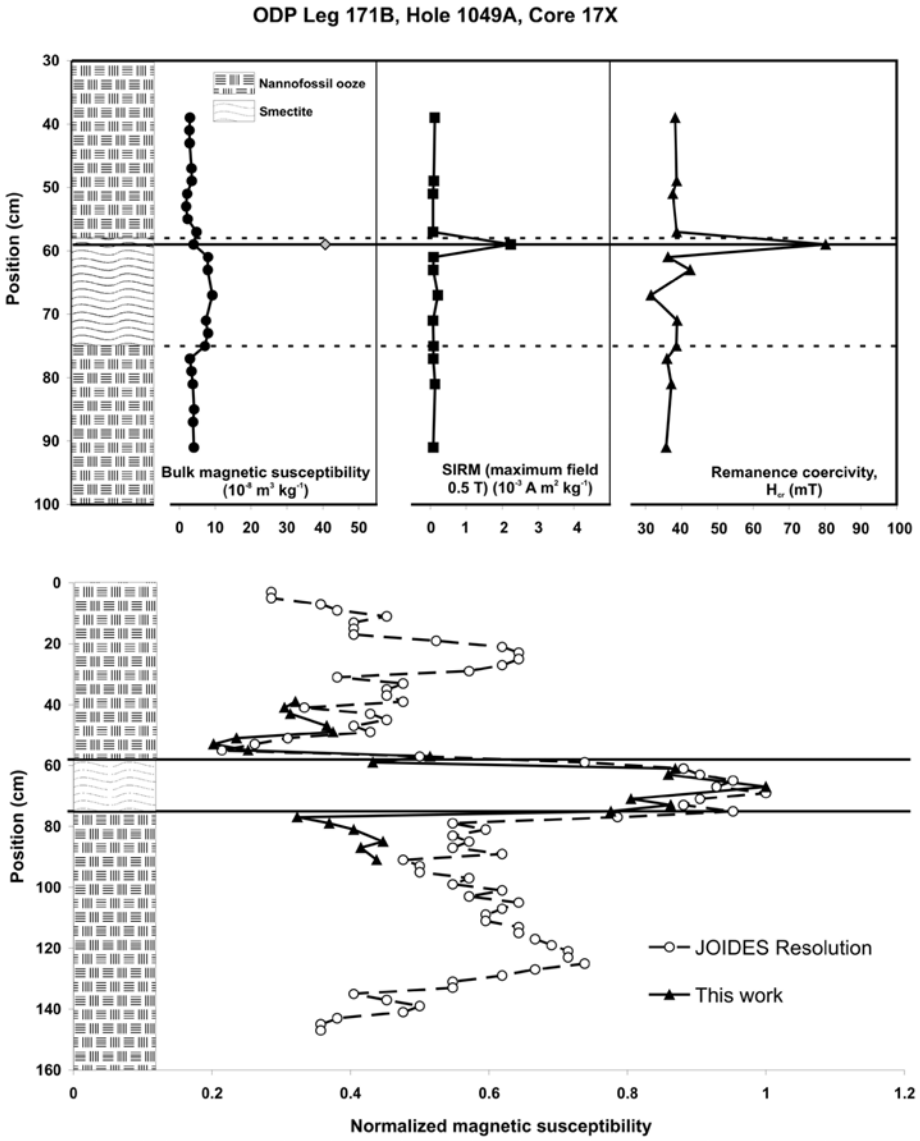

Fig. 10. Top: Magnetic properties across K-T boundary at ODP Hole 1049A, with grey rhombus in the susceptibility profile representing just the limonitic layer; the SIRM and H_{cr} profiles include at that position data for just the limonitic layer. Bottom: comparison of ODP Hole 1049A susceptibility profiles obtained in this work and measured by the on-board JOIDES Resolution Team, normalized by maximum values.

susceptibility, correlated with a similar increase in SIRM and with a very high value of remanence coercivity, is observed in the reddish layer placed on top of the sandstone beds. Although some variations are observed within and between the other lithologies, that spike stands alone, not so much because of its intensity (observe the downward increase in susceptibility and SIRM values for Mendez marls, which even surpass the reddish layer spike values), but mostly because the extraordinarily high values of H_{cr}. Figure 14 (top) shows the IRM acquisition curves for all Mimbral samples. All the lithologies (marls, spherule bed, sandstones, and clay-rich interval) present a very similar behavior, dominated by a low-coercivity phase, presumably magnetite, with minor contribution from high-coercivity phases. However, the reddish layer curve is quite different: no low-coercivity phase is present, but rather a magnetic phase with very high remanence coercivity dominates. This high-coercivity phase presents, as in the case of ODP Hole 1049A limonitic layer and Agost Fe-O spherules, significant IRM relaxation (Fig. 14, bottom), pointing to very fine grain sizes.

In La Lajilla a more complex behavior is detected. First, in this section, no reddish clay-rich layer is visually defined on top of the sandstones and no susceptibility spike is observed in this place. But, very interestingly, a clear spike in SIRM and a very high value of remanence coercivity is present at a stratigraphic position slightly higher to that of the spike detected in El Mimbral (Fig. 13). In fact, the H_{cr} value is even higher in La Lajilla than El Mimbral. This high-

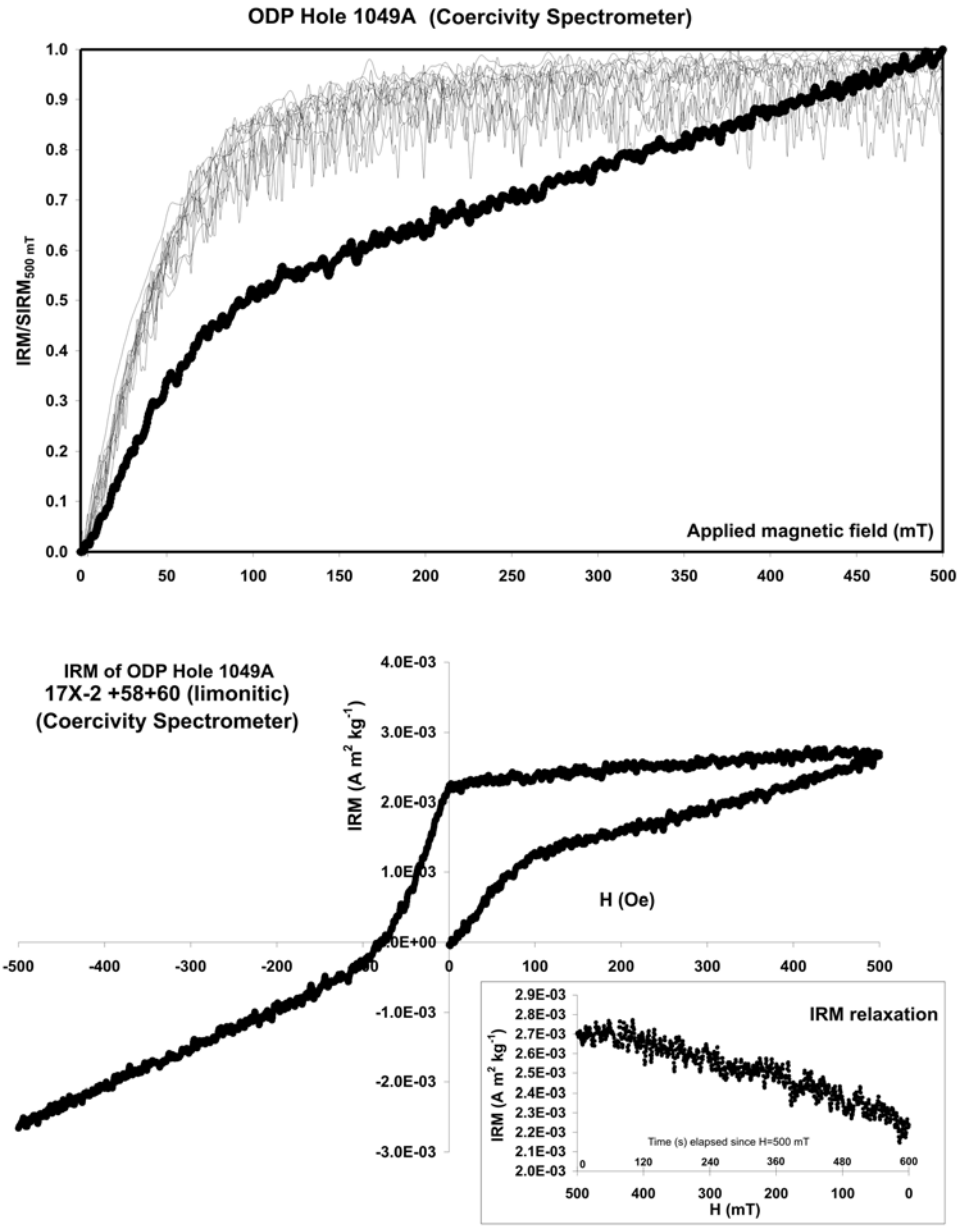

Fig. 11. Top: IRM acquisition curves for ODP Hole 1049A samples; black circles correspond to limonitic layer; thin lines correspond to the rest of the samples, both Cretaceous and Tertiary nanofossil ooze and K-T boundary smectite layer. Bottom: IRM acquisition and back-demagnetization for ODP Hole 1049A limonitic layer, with IRM relaxation in the inset.

coercivity phase, present both in El Mimbral and La Lajilla at similar stratigraphic positions and corresponding in El Mimbral to the reddish layer, can be identified by its high H_{cr} values and IRM acquisition and demagnetization curves as goethite with fine grain sizes, a significant fraction of which show superparamagnetic behavior. In La Lajilla this high coercivity spike is not unique. In general, the remanence coercivities of La Lajilla spherule bed samples are also very high, and increases in SIRM are also observed. The behavior of these samples is not homogeneous, with several and alternating ups and downs in both parameters. Another important point is that the highest values of SIRM and remanence coercivity within the spherule bed are coincident with the stratigraphic contacts with Mendez marls and sandstone beds, where reddish postdepositional features were observed. This information places a strong suspicion on the high-coercivity phases in the spherule bed as being produced by postdepositional alteration.

In Fig. 14 (bottom), the IRM acquisition curves for all La Lajilla samples are plotted. The different behaviors of different lithologies are clear. Mendez marls, sandstones, clay-rich interval, and Velasco marls behave in an almost identical

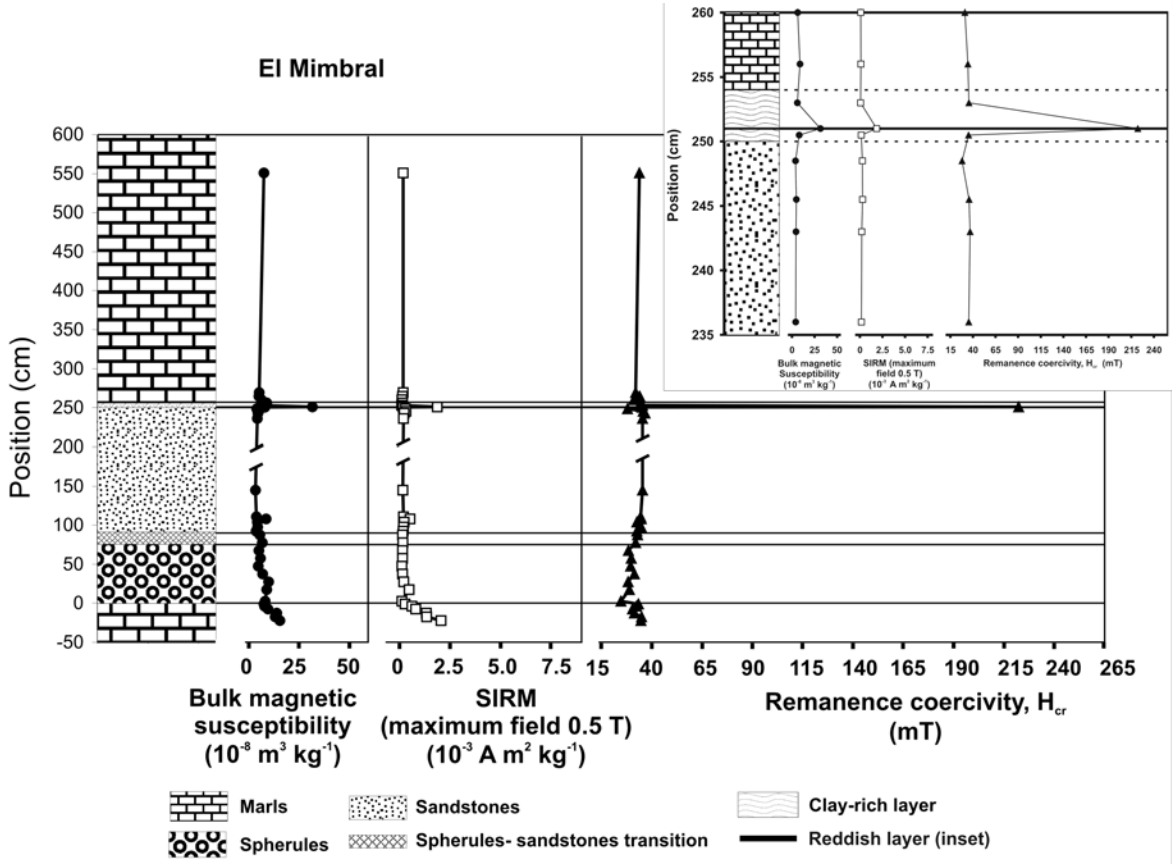

Fig. 12. Magnetic properties across K-T boundary at El Mimbral. Inset: Zoom on the upper stratigraphic position corresponding to the transition between sandstones and Velasco marls.

way, with a low-coercivity phase (probably detrital magnetite) dominating the magnetization and minor contributions from higher coercivity phases. Samples from the spherule bed show much higher coercivities and saturation fields and minor or no low-coercivity contribution. The transition between spherule and sandstone beds shows a low-coercivity contribution slightly more important than the rest of the spherule bed, but is still clearly dominated by high-coercivity phases. And finally, the two samples from the lowermost Velasco marls that show the remanence coercivity spike in Fig. 13 are also dominated by high-coercivity phases. Notably, the two samples with the highest remanence coercivities, which show no low-coercivity contribution and which are almost identical, are the one from the bottom of the spherule bed, with reddish postdepositional alteration, and the one from the low part of the Velasco marls that shows the spike in SIRM and H_{cr}. Their similar IRM behavior is shown in Fig. 14 (bottom), where the IRM relaxation pattern can also be appreciated.

Geochemistry

The geochemical profiles from El Mimbral are plotted in Fig. 15, where some major and trace element abundances are shown. Normalization by Al concentration was performed in most of the cases to avoid differences due to carbonate content. Figure 16 shows the same data, but centered on the upper part of the stratigraphic column. Platinum group elements (PGE) abundances are plotted in Fig. 17. Iridium is plotted alone in Fig. 18. These data are indicative of a terrestrial origin of the materials in the section, with a small extraterrestrial contribution within the lowermost Velasco marls, as denoted by iridium. Small increments in the abundance of some elements are detected at the base of the spherule bed and in the lower part of the sandstones. Note, for example, the increase in Ca content at the base of the spherules, probably related to calcite concretions observed within this highly altered layer.

In the upper part, a small increase in Al coupled with Sr can be seen at 256 cm (lower Velasco marls), as well as increases in Fe, Mg, V, Mo, and Pb just in the reddish layer (251 cm) where the high-remanence coercivity magnetic spike is detected. Ten centimeters higher (around 265 cm), an increase in Ba content is apparent, pointing to a diagenetic remobilization scenario. The other elements behave more or less uniformly with typical terrestrial concentrations, including Ni, Co, and Cr. The reddish layer is also enriched in some PGE (Au and Pt), but the others show small increases above this layer. Iridium reaches the highest value (0.88 ppb)

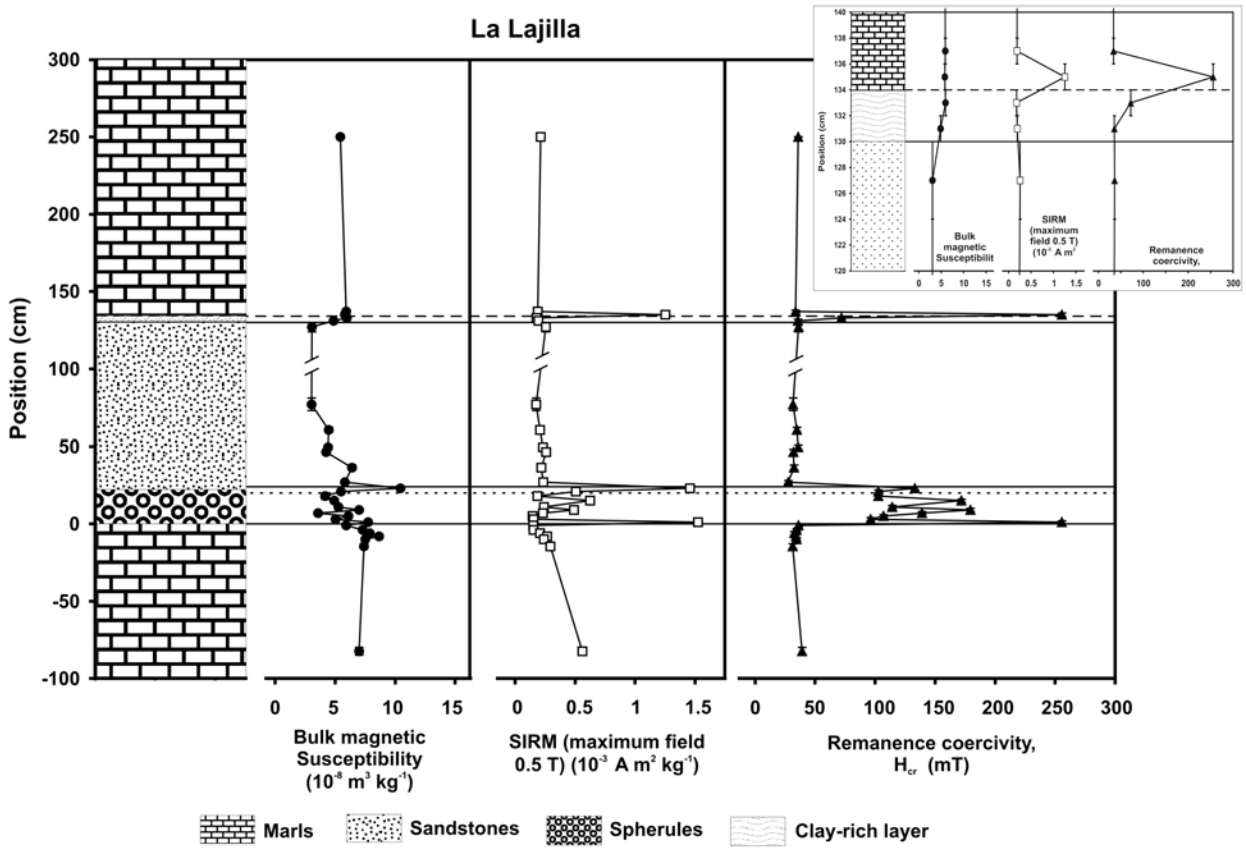

Fig. 13. Magnetic properties across K-T boundary at La Lajilla. Inset: Zoom on the upper stratigraphic position corresponding to the transition between sandstones and Velasco marls.

at 256 cm, 4 cm above the reddish layer, although the abundance within this layer, being low, is slightly higher than the background values, which fall below the instrumental detection limit of 0.04 ppb. Palladium and Ru behave in the same way. Therefore, the iridium data show a small enrichment in extraterrestrial material within the lower centimeters of the Velasco marls, which is in agreement with López-Oliva and Keller (1996) and Keller et al. (1997). This enrichment is not coupled with the Fe and magnetic spike at the reddish layer, which lies several centimeters below the iridium maximum.

The geochemical data from El Mimbral resemble that from Blake Nose (Martínez-Ruiz et al. 2001b). In both sections, a reddish Fe-rich layer, several millimeters thick, is observed on top of the K-T boundary material. In Blake Nose it lies just on top of the spherule bed. In El Mimbral, it lies on top of the sandstones that separate the spherule bed from the lowermost Tertiary marls. In both cases, the reddish layer show no significant enrichment in extraterrestrial component, but an iridium spike is observed some centimeters above the layer, mixed with the lowermost Danian sediments. Again in both cases, barium behavior and uncoupled peaks of different elements point strongly to diagenetic remobilization as responsible of at least some of the enrichments.

DISCUSSION AND CONCLUSIONS

The results described in the previous pages lead us to significant conclusions. In the Agost and Caravaca sections, the K-T boundary fireball layer is connected with a clear magnetic spike consisting of high mass-susceptibility and SIRM values, low-remanence coercivity, transformation and unblocking temperatures between 250 and 450 °C, and no Verwey transition. The Agost Fe-O spherules behave as a mixture of a low-remanence coercivity phase, with similar transformation temperatures, and a high coercivity component that can be identified as goethite. The SIRM relaxation shown by this goethite points to an important superparamagnetic fine-grained fraction. As the bulk sample, the spherules show no Verwey transition. Therefore, a pure magnetite composition of the low-remanence coercivity phase can be discarded both for the bulk sample and the Fe-O spherules, eliminating the single-domain magnetite reported by Griscom et al. (1999) as a viable candidate to explain the fireball layer magnetic signature. Equally, there is not any trace of the low-Ni iron spherules reported by Morden (1993) in Stevns Klint. Considering that the Fe-O spherules have lower mass-susceptibility and SIRM than the bulk sample, and that Caravaca behaves identically even when no Fe-O

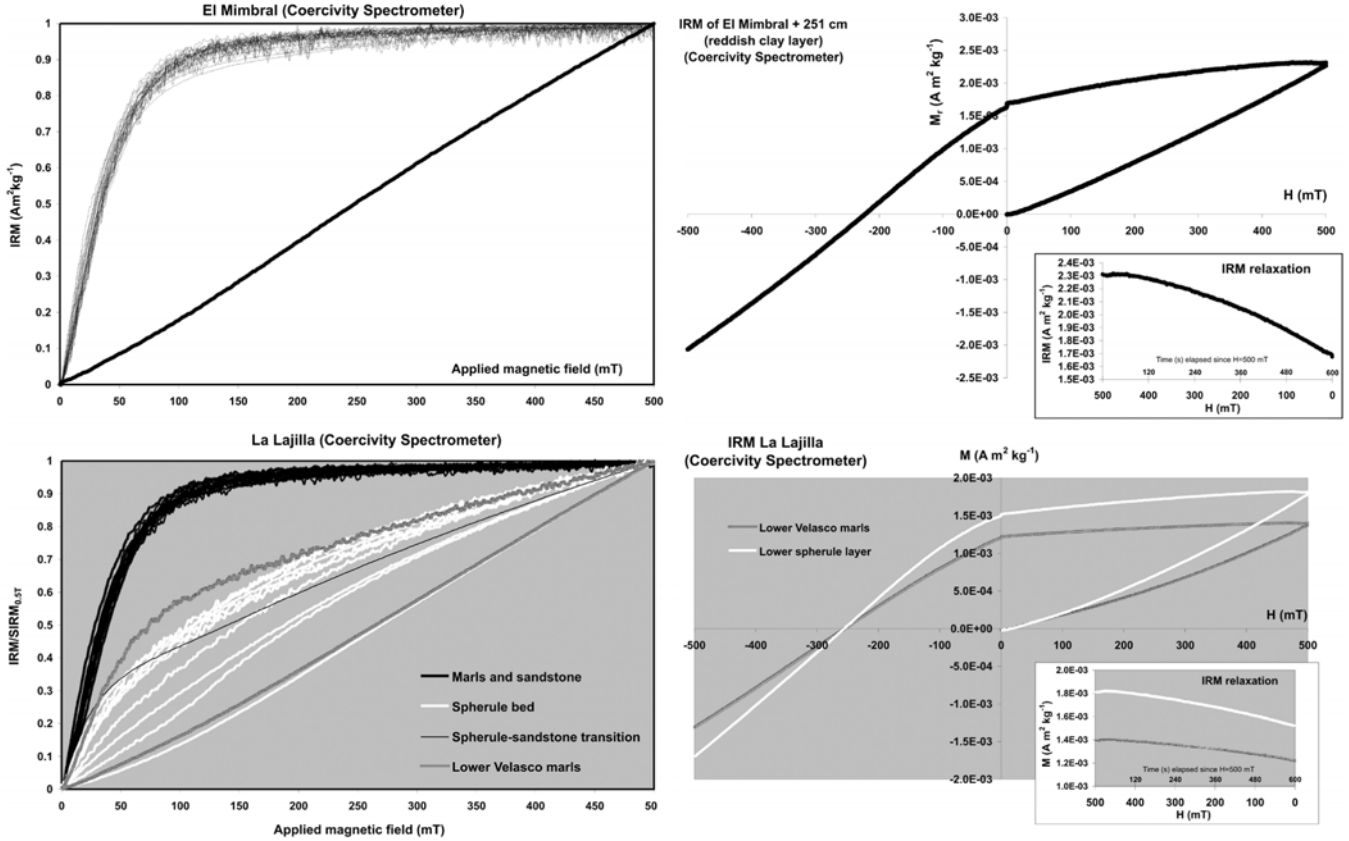

Fig. 14. Left: IRM acquisition curves for El Mimbral (top) and La Lajilla (bottom) samples. Right: IRM acquisition and back-demagnetization curves for the high coercivity samples, with IRM relaxation in the insets, both for El Mimbral (top) and La Lajilla (bottom).

spherules are present there, it can be concluded that the magnetic phase responsible of the characteristics of the fireball layer is not exclusively concentrated within the spherules, but is mainly dispersed through the fine fraction of the sediment.

These magnetic properties are compatible with, and indeed point strongly to, highly oxidized magnesium and nickel-rich spinel crystallites as the mineral responsible of the characteristic low-remanence coercivity magnetic phase. Cation substitution in magnetite, especially by Mg, Al, and Cr, is known to decrease Curie temperatures. This cation substitution and the high oxidation state explain the observed IRM unblocking temperatures below 450 °C, the irreversible character of the thermomagnetic curves, and the total absence of Verwey transition. The high oxidation state typical of K-T boundary magnesioferrites has been extensively studied (Smit and Kyte 1984; Kyte and Smit 1986; Robin et al. 1992; Gayraud et al. 1996; Ebel and Grossman 2005) and recognized, together with high Ni content, as an indication of their origin from meteoritic material travelling deeply into the Earth's atmosphere, where high oxygen fugacities can be obtained. Following the prevailing view, the Ni-rich spinels would have originated as high-temperature phases crystallized in the interior of melt droplets. These droplets condensed directly from the impact vapor cloud (Bohor et al. 1986; Ebel and Grossman 2005) or formed as ablation products from meteoritic fragments travelling through the Earth's atmosphere (Robin et al. 1992; Gayraud et al. 1996). These Ni-rich spinels or magnesioferrites were reported in Caravaca by Bohor et al. (1986), Robin et al. (1991), and Kyte and Bostwick (1995), where they are present as free crystallites diluted in the clay matrix. In other sections, the magnesioferrites are reported to be concentrated within the microspherules (Montanari et al. 1983; Smit and Kyte 1984; Kyte and Smit 1986). According to the magnetic data, in Agost most of these crystallites must be also diluted in the smectite matrix, but possibly a fraction of them is still embedded in the surviving Fe-O spherules. This is very different from the results obtained by Worm and Banerjee (1987) and Cisowski (1988) in Petriccio section, where the magnetic properties were concentrated in the spherules and the matrix showed much lower susceptibility and saturation magnetization. This difference between the Italian and Iberian sections is probably due to differences in the diagenetic history they experienced. Indeed, in Agost and Caravaca, the original material composing the spherules was almost totally altered or replaced by diagenesis (Martínez-Ruiz 1994; Martínez-Ruiz et al. 1997, 1999), and differences in redox

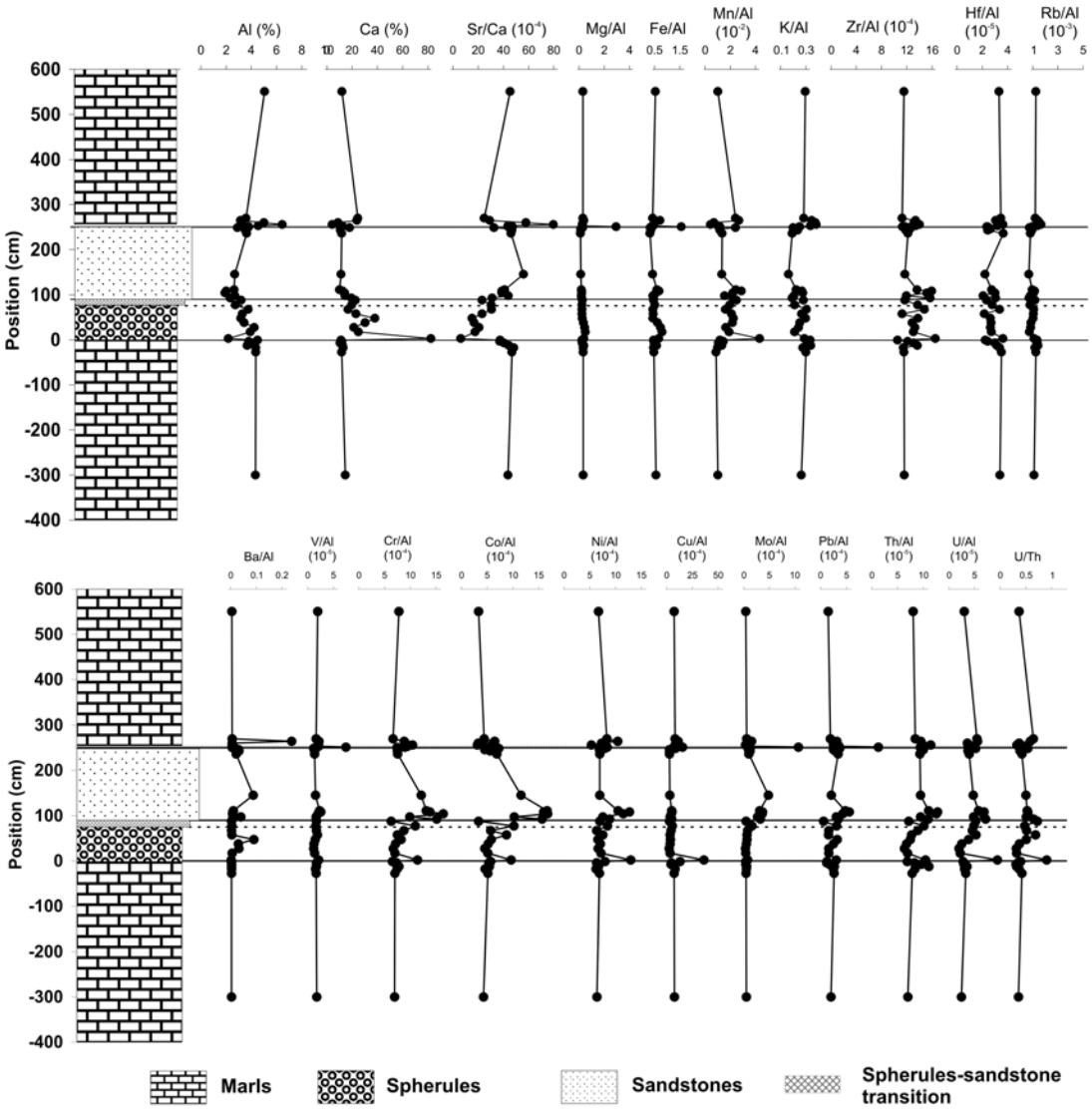

Fig. 15. Geochemical profiles from the K-T boundary interval at El Mimbral. Profiles show Ca and Al concentrations, the Sr/Ca ratio, and several element concentrations normalized to Al versus depth.

conditions during diagenesis led to different assemblages of spherules in Caravaca and Agost, with no Fe-O spherules in the former. The Ni-rich spinels, being much more resistant to alteration, survived their host spherules and remain dispersed in the fine fraction. This diagenetic alteration explains also the presence of very fine-grained goethite in Agost Fe-O spherules as an authigenic product. Comparing Agost and Caravaca thermomagnetic behavior with the curves reported by Cisowski (1988) for Petriccio, similar transformation/unblocking temperatures are obtained in the three sections. Therefore, magnetic data would point to broadly similar Mg and Ni-rich spinels composition in the three sections. Nevertheless, detailed studies by Kyte and Bostwick (1995) and Robin and Rocchia (1998) have shown significant differences in Ni-rich spinel composition between Caravaca on one side, and Petriccio and Furlo (both in Italy) on the other. This difference, mainly a much higher Cr content in Caravaca spinels, is not clearly reflected in the magnetic data, revealing a relative insensitivity of unblocking/transformation temperatures to the reported range of spinel composition variation.

At closer (Blake Nose) and proximal (El Mimbral and La Lajilla) sections, the situation revealed by the magnetic properties and the geochemistry is very different. First, there is no indication of the presence of the low remanence coercivity magnetic phase characteristic of the fireball layer at distal sections, identified as Mg and Ni-rich spinels. Since these spinels have indeed been detected both in El Mimbral (Rocchia et al. 1996) and La Lajilla (Bohor 1996), an explanation for the absence of their magnetic signature is needed. There are two arguments that can help explain this. First, while in distal sections, all the extraterrestrial input is

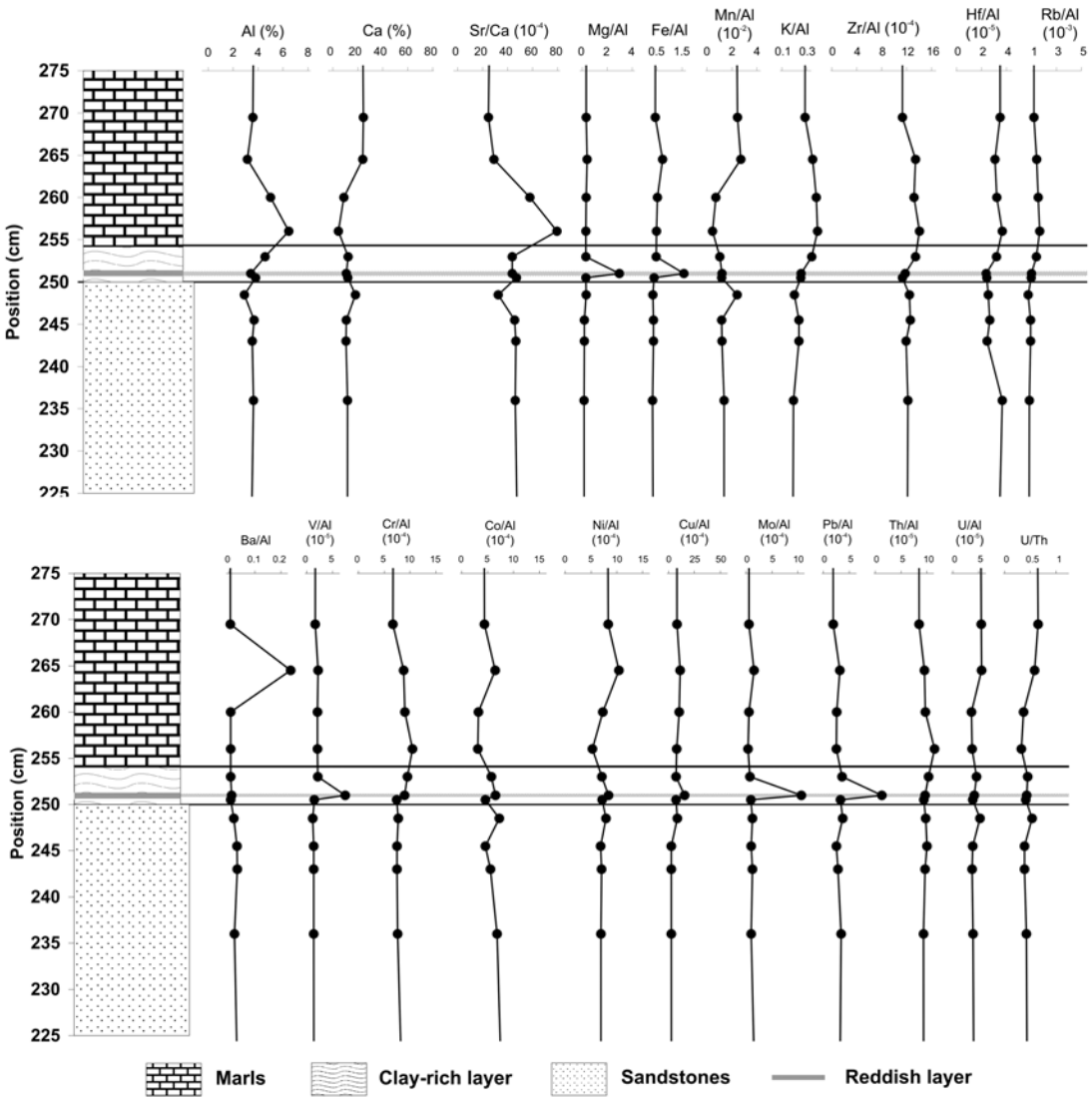

Fig. 16. El Mimbral geochemical profiles, zoom on the upper stratigraphic position corresponding to the transition between sandstones and Velasco marls.

concentrated in the very thin (2 mm) fireball layer, near the Chicxulub crater the sedimentary expression of the impact event consists of a much thicker set, a lower bed rich in spherules coming mainly from the target material and an upper bed several centimeters thick of fine material enriched in the extraterrestrial component. Thus, dilution of the meteoritic fraction is much higher in proximal sections and its magnetic properties can be obliterated by the rest of the material in the sample. Additionally, during the impact process, the mass coming from the impactor is expected to attain the highest kinetic energy, and thus the proximal ejecta are thought to contain a relative higher fraction of low kinetic energy terrestrial target material, while the impact vapor cloud and distal ejecta will be highly enriched in meteoritic material (Smit 1999; Martínez-Ruiz et al. 2006). These differences between distal and proximal sections are expressed in differences in the concentrations of the extraterrestrial components. While Ir maximum reaches 24.4 ppb in Agost (Martínez-Ruiz et al. 1992) and 35.2–52 ppb in Caravaca (Martínez-Ruiz 1994; Bohor et al. 1986), it is only 1.32 ppb in ODP Hole 1049A (Smit et al. 1997; Martínez-Ruiz et al. 2001b) and 0.88 ppb in El Mimbral. Regarding Ni-rich spinels, maximum concentration in Caravaca is about $2 \cdot 10^5$ spinels/g (Robin et al. 1991), while it is only 300 spinels/g in El Mimbral (Rocchia et al. 1996), and just some rare crystals in La Lajilla (Bohor 1996). In Blake Nose, no spinels are reported in the literature. This scarcity of Ni-rich spinels in closer and proximal sections is reflected (or more accurately, is not reflected) in the magnetic properties, indicating that the boundary material from these sections is mainly of terrestrial origin. Let us compare the two cases where

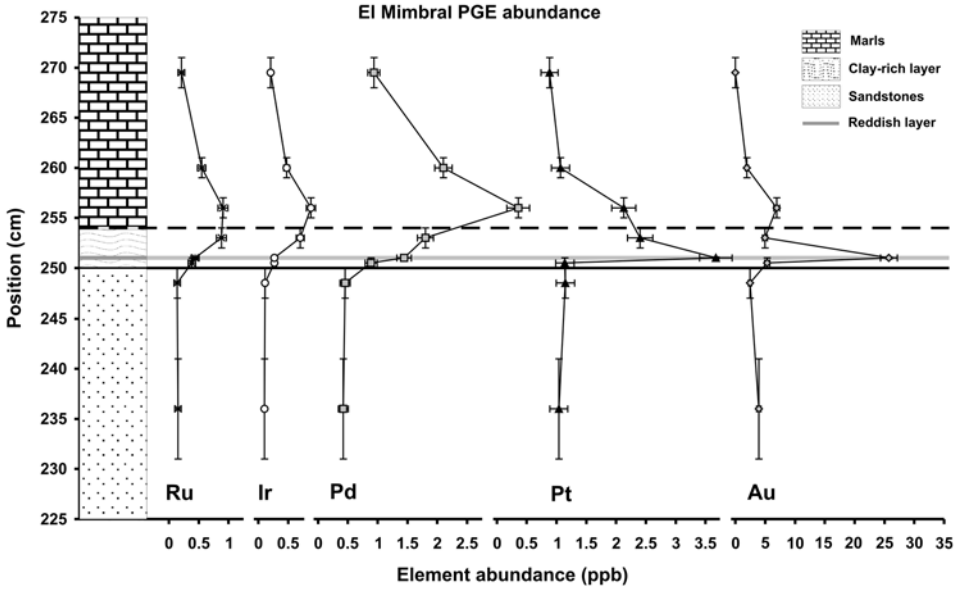

Fig. 17. Platinum group elements (PGE) abundances for El Mimbral at the transition between sandstones and Velasco marls. Estimated error bars (2σ) for each measured concentration are also plotted. Instrumental detection limits in ppb are: Ru 0.13; Ir 0.04; Pd 0.11; Pt 0.14; Au 0.71.

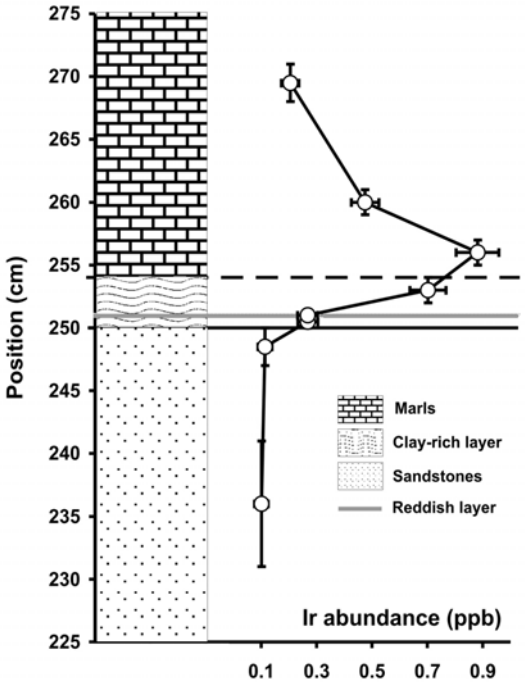

Fig. 18. Iridium abundance and estimated error bars (2σ) at El Mimbral transition between sandstones and Velasco marls. The instrumental detection limit is 0.04 ppb.

quantitative data is available: in Caravaca, with $2{\cdot}10^5$ spinels/g, the susceptibility and SIRM values of the fireball layer are one order of magnitude higher than in Cretaceous and Tertiary surrounding material. This implies that, if spinel abundance drops one order of magnitude, its magnetic signal would be not enough to overrun that of the matrix material. This is what happens in El Mimbral, where the maximum abundance of Ni-rich spinels ($3{\cdot}10^2$ spinels/g) is not one but three orders of magnitude lower than in Caravaca. An important conclusion is that magnetic properties strongly support the relative distribution pattern of the impact-derived materials, indicating the contribution of extraterrestrial materials.

The second important result regarding closer and proximal sections is the presence of a layer rich in fine-grained goethite on top of the siliciclastic pack (El Mimbral and La Lajilla) and the smectite-rich spherule layer (ODP Hole 1049A) that mark the K-T boundary impact event. The position of this goethite layer coincides more or less with the stratigraphic position where the fine fraction of the impact-derived material is expected to have settled, but great attention must be focused on the details before assuming it as a meteoritic product. In Blake Nose, this goethite-rich layer has previously been shown as likely having a diagenetic origin (Martínez-Ruiz et al. 2001b): it does not contain maximum Ir concentrations, it does not show significant geochemical anomalies, and also considering that diagenetic remobilization in a reducing environment is deduced from the geochemical data. A similar situation is found in El Mimbral: the goethite-rich layer does not show abnormal increases in extraterrestrial tracers, the Ir maximum is detected some centimeters above this layer within the lowermost centimeters of the first Tertiary marls, and there is geochemical indication of diagenetic remobilization. Moreover, in La Lajilla, fine-grained goethite with identical magnetic properties is found at other stratigraphic positions within the spherule bed that is rich in reddish altered material, and especially in its contacts

with under and overlaying beds. Additionally, the magnetic behavior of this goethite is close to that of the high-coercivity magnetic phase observed in Agost Fe-O spherules, where diagenetic replacement of original material has taken place. The previous considerations point to a diagenetic origin of this fine-grained goethite. Under the unusual redox conditions imposed by the impact event itself, with the huge mass-waste delivery that affected the Blake Nose and proximal sections studied here and the subsequent mass-mortality and organic material deposition, we can expect diagenetic remobilization and reprecipitation of elements. A similar scenario was proposed by Brooks et al. (1985) to explain the iron phases described in Woodside Creek (see the Introduction). Whether the iron precipitated in these goethite-rich layers has a primary meteoritic origin and was remobilized and reprecipitated afterward, or whether it originated authigenically after the impact due to diagenetic conditions is something that can not be definitely answered with the magnetic and geochemical data presented in this work. However, the authors think that the data presented here denies this fine-grained goethite as the iridium carrier (as has been proposed by Wdowiak et al. 2001), and raises serious doubts about its proposed meteoritic origin.

Acknowledgments–The authors of this paper are grateful to the staff of the Paleomagnetic Laboratory of ETH, Zürich (Switzerland) for their help during some experiments; to Danis Nourgaliev and Pavel Iassonov, Kazan University, for the measurement of Agost Fe-O spherules thermomagnetic curve; to J. C. Gómez-Sal and colleagues, Universidad de Cantabria, for their facilities and help during low-temperature measurements; to Belén Soutullo, Universidad Complutense de Madrid, for the X-ray diffraction measurements; to the Ocean Drilling Program for samples from Leg 171B, Hole 1049A; to Guillermo Villasante for his help during fieldwork in southern Spain; to Lucía Lozano for her support in Mexico; to Pedro Arredondo (Instituto de Geología, Universidad Nacional Autónoma de México) for his invaluable help during fieldwork in northeastern Mexico; and finally to Eric Robin and Frank Kyte for their constructive reviews.

Editorial Handling—Dr. Elisabetta Pierazzo

REFERENCES

Alegret L., Molina E., and Thomas E. 2001. Benthic foraminifera at the Cretaceous-Tertiary boundary around the Gulf of México. *Geology* 29:891–894.

Alegret L., Arenillas I., Arz J. A., Liesa C., Melendez A., Molina E., Soria A. R., and Thomas E. 2002. The Cretaceous/Tertiary boundary: Sedimentology and micropaleontology at El Mulato section, NE Mexico. *Terra Nova* 14:330–336.

Alvarez L. W., Alvarez W., Asaro F., and Michel H. V. 1980. Extraterrestrial cause for the Cretaceous-Tertiary extinction. *Science* 208:1095–1108.

Arz J. A., Arenillas I., Soria A. R., Alegret L., Grajales-Nishimura J. M., Liesa C. L., Melendez A., Molina E., and Rosales M. C. 2001. Micropaleontology and sedimentology across the Cretaceous/Tertiary boundary at La Ceiba (Mexico): Impact-generated sediment gravity flows. *Journal of South American Earth Sciences* 14:505–519.

Bhandari N., Verma H. C., Upadhyay C., Tripathi A., and Tripathi R. P. 2002. Global occurrence of magnetic and superparamagnetic iron phases in Cretaceous-Tertiary boundary clays. In *Catastrophic events and mass extinctions: Impacts and beyond*, edited by Koeberl C. and MacLeod K. G. GSA Special Paper #356. Boulder, Colorado: Geological Society of America. pp. 201–211.

Bohor B. F. 1996. A sediment gravity flow hypothesis for siliciclastic units at the K/T boundary, northeastern Mexico. In *The Cretaceous-Tertiary boundary event and other catastrophes in Earth history*, edited by Ryder G., Fastovsky D., and Gartner S. GSA Special Paper #307. Boulder, Colorado: Geological Society of America. pp. 183–195.

Bohor B. F., Foord E. E., Modreski P. J., and Triplehorn D. M. 1984. Mineralogic evidence for an impact event at the Cretaceous-Tertiary event. *Science* 224:867–869.

Bohor B. F., Foord E. E., and Ganapathy R. 1986. Magnesioferrite from the Cretaceous-Tertiary boundary, Caravaca, Spain. *Earth and Planetary Science Letters* 81:57–66.

Bohor B. F., Modreski P. J., and Foord E. E. 1987. Shocked quartz in the Cretaceous-Tertiary boundary clays: Evidence for a global distribution. *Science* 236:705–709.

Bralower T. J., Paull Ch. K., and Leckie R. M. 1998. The Cretaceous-Tertiary boundary cocktail: Chicxulub impact triggers margin collapse and extensive sediment gravity flows. *Geology* 26:331–334.

Brooks R. R., Hoek P. L., Reeves R. D., Wallace R. C., Johnston J. H., Ryan D. E., Holzbecher J., and Collen J. D. 1985. Weathered spheroids in a Cretaceous/Tertiary boundary shale at Woodside Creek, New Zealand. *Geology* 13:738–740.

Burov B. V., Nourgaliev D. K., and Iassonov P. G. 1986. *Paleomagnetic analysis.* Kazan, Russia: Kazan University Press. 176 p.

Cisowski S. M. 1988. Magnetic properties of K/T and E/O microspherules: Origin by combustion? *Earth and Planetary Science Letters* 88:193–208.

Cisowski S. M. 1990. The significance of magnetic spheroids and magnesioferrite occurring in K/T boundary sediments. In *Global catastrophes in Earth history: An interdisciplinary conference on impacts, volcanism and mass mortality*, edited by Sharpton V. L. and Ward P. D. GSA Special Paper #247. Boulder, Colorado: Geological Society of America. pp. 359–365.

Claeys Ph., Kiessling W., and Alvarez W. 2002. Distribution of Chicxulub ejecta at the Cretaceous-Tertiary boundary. In *Catastrophic events and mass extinctions: Impacts and beyond*, edited by Koeberl C. and MacLeod K. G. GSA Special Paper #356. Boulder, Colorado: Geological Society of America. pp. 55–68.

D'Hondt S., King J., and Gibson C. 1996. Oscillatory marine response to the Cretaceous-Tertiary impact. *Geology* 24:611–614.

Dunlop D. J. and Özdemir Ö. 1997. *Rock magnetism: Fundamentals and frontiers*. Cambridge: Cambridge University Press. 573 p.

Ebel D. S., and Grossman L. 2005. Spinel-bearing spherules condensed from the Chicxulub impact-vapor plume. *Geology* 33: 293–296.

Ganapathy R. 1980. A major meteorite impact on the Earth 65 million years ago: Evidence from the Cretaceous-Tertiary boundary clay. *Science* 209:921–923.

Gayraud J., Robin E., Rocchia R., and Froget L. 1996. Formation

conditions of oxidized Ni-rich spinel and their relevance to the K/T boundary event. In *The Cretaceous-Tertiary boundary event and other catastrophes in Earth history*, edited Ryder G., Fastovsky D., and Gartner S. GSA Special Paper #307. Boulder, Colorado: Geological Society of America. pp. 425–443.

Griscom D. L., Beltran-Lopez V., Merzbacher C. I., and Bolden E. 1999. Electron spin resonance of 65-million-year-old glasses and rocks from the Cretaceous-Tertiary boundary. *Journal of Non-Crystalline Solids* 253:1–22.

Keller G., Stinnesbeck W., and Lopez-Oliva J. G. 1994. Age, deposition and biotic effects of the Cretaceous/Tertiary boundary event at Mimbral, NE Mexico. *Palaios* 9:144–157.

Keller G., Lopez-Oliva J. G., Stinnesbeck W., and Adatte T. 1997. Age, stratigraphy, and deposition of near K/T siliciclastic deposits in Mexico: Relation to bolide impact? *GSA Bulletin* 109: 410–428.

Klaus A., Norris R. D., Kroon D., and Smit J. 2000. Impact-induced mass wasting at the K-T boundary: Blake Nose, western North Atlantic. *Geology* 28:319–322.

Kyte F. T. 2002. Tracers of the extraterrestrial component in sediments and inferences for Earth's accretion history. In *Catastrophic events and mass extinctions: Impacts and beyond*, edited by Koeberl C. and MacLeod K. G. GSA Special Paper #356. Boulder, Colorado: Geological Society of America. pp. 21–38.

Kyte F. T. and Bostwick J. A. 1995. Magnesioferrite spinel in Cretaceous/Tertiary boundary sediments of the Pacific basin: Remnants of hot, early ejecta from the Chicxulub impact? *Earth and Planetary Science Letters* 132:113–127.

Kyte F. T. and Smit J. 1986. Regional variations in spinel compositions: An important key to the Cretaceous/Tertiary event. *Geology* 14:485–487.

Kyte F. T., Zhou Z., and Wasson J. T. 1980. Siderophile-enriched sediments from the Cretaceous-Tertiary boundary. *Nature* 288: 651–656.

Lawton T. F., Shipley K. W., Aschoff J. L., Giles K. A., and Vega F. J. 2005. Basinward transport of Chicxulub ejecta by tsunami-induced backflow, La Popa basin, northeastern Mexico, and its implications for distribution of impact-related deposits flanking the Gulf of Mexico. *Geology* 33:81–84.

Lopez-Oliva J. G. and Keller G. 1996. Age and stratigraphy of near-K/T boundary siliciclastic deposits in northeastern Mexico. In *The Cretaceous-Tertiary boundary event and other catastrophes in Earth history*, edited by Ryder G., Fastovsky D., and Gartner S. GSA Special Paper #307. Boulder, Colorado: Geological Society of America. pp. 227–242.

Lowrie W. 1990. Identification of ferromagnetic minerals in a rock by coercivity and unblocking temperature properties. *Geophysical Research Letters* 17:159–162.

Luck J. M. and Turekian K. K. 1983. Osmium-187/Osmium-186 in Manganese nodules and the Cretaceous-Tertiary boundary. *Science* 222:613–615.

Martínez-Ruiz F. 1994. Geoquímica y mineralogía del tránsito Cretácico-Terciario en las Cordilleras Béticas y en la Cuenca Vasco-Cantábrica. Ph.D. thesis, University of Granada, Granada, Spain.

Martinez-Ruiz F., Ortega-Huertas M., Palomo I., and Barbieri M. 1992. The geochemistry and mineralogy of the Cretaceous-Tertiary boundary at Agost (southeast Spain). *Chemical Geology* 95:265–281.

Martinez-Ruiz F., Ortega-Huertas M., Palomo I., and Acquafredda P. 1997. Quench textures in altered spherules from the Cretaceous-Tertiary boundary layer at Agost and Caravaca, SE Spain. *Sedimentary Geology* 113:137–147.

Martinez-Ruiz F., Ortega-Huertas M., and Palomo I. 1999. Positive Eu anomaly development during diagenesis of the K/T boundary ejecta layer in the Agost section (SE Spain): Implications for trace-element remobilization. *Terra Nova* 11:290–296.

Martinez-Ruiz F., Ortega-Huertas M., Palomo-Delgado I., and Smit J. 2001a. K-T boundary spherules from Blake Nose (ODP Leg 171B) as a record of the Chicxulub ejecta deposits. In *Western North Atlantic Paleogene and Cretaceous palaeoceanography*, edited by Kroon D., Norris R. D., and Klaus A. Geological Society of London Special Publication #183. London, UK. pp. 149–161.

Martinez-Ruiz F., Ortega-Huertas M., Kroon D., Smit J., Palomo-Delgado I., and Rocchia R. 2001b. Geochemistry of the Cretaceous-Tertiary boundary at Blake Nose (ODP Leg171B). In *Western North Atlantic Paleogene and Cretaceous palaeoceanography*, edited by Kroon D., Norris R. D., and Klaus A. Geological Society of London Special Publication #183. London, UK. pp. 131–148.

Martinez-Ruiz F., Ortega-Huertas M., and Rivas P. 2006. Rare earth element composition as evidence of the precursor material of Cretaceous-Tertiary boundary sediments at distal sections. *Chemical Geology* 232:1–11.

Montanari A., Hay R. L., Alvarez W., Asaro A., Michel H. V., and Alvarez L. W. 1983. Spheroids at the Cretaceous-Tertiary boundary are altered impact droplets of basaltic composition. *Geology* 11:668–671.

Morden S. J. 1993. Magnetic analysis of K/T boundary layer clay from Stevns Klint, Denmark. *Meteoritics* 28:595–599.

Norris R. D., Kroon D., Klaus A., et al., editors. 1998. Proceedings of the Ocean Drilling Program. Initial report #171B. College Station, Texas: Ocean Drilling Program. pp. 321–347.

Robin E. and Rocchia R. 1998. Ni-rich spinel at the Cretaceous-Tertiary boundary of El Kef, Tunisia. *Bulletin de la Société géologique de France* 169:365–372.

Robin E., Boclet D., Bonte Ph., Froget L., Jehanno C., and Rocchia R. 1991. The stratigraphic distribution of Ni-rich spinels in Cretaceous-Tertiary boundary rocks at El Kef (Tunisia), Caravaca (Spain), and Hole 761C (Leg 122). *Earth and Planetary Science Letters* 107:715–721.

Robin E., Bonte Ph., Froget L., Jehanno C., and Rocchia R. 1992. Formation of spinels in cosmic objects during atmospheric entry: A clue to the Cretaceous-Tertiary boundary event. *Earth and Planetary Science Letters* 108:181–190.

Rocchia R., Robin E., Froget L., and Gayraud J. 1996. Stratigraphic distribution of extraterrestrial markers at the Cretaceous-Tertiary boundary in the Gulf of Mexico area: Implications for the temporal complexity of the event. In *The Cretaceous-Tertiary boundary event and other catastrophes in Earth history*, edited by Ryder G., Fastovsky D. and Gartner S. GSA Special Paper #307. Boulder, Colorado: Geological Society of America. pp. 279–286.

Sharpton V. L., Dalrymple G. B., Marin L. E., Ryder G., Schuraytz B. C., and Urrutia-Fucugauchi J. 1992. New links between the Chicxulub impact structure and the Cretaceous/Tertiary boundary. *Nature* 359:819–821.

Shukolyukov A. and Lugmair G. W. 1998. Isotopic evidence for the Cretaceous-Tertiary impactor and its type. *Science* 282:927–929.

Sigurdsson H., D'Hondt S., Arthur M. A., Bralower T. J., Zachos J. C., Van Fossen M., and Channell J. E. T. 1991. Glass from the Cretaceous/Tertiary boundary in Haiti. *Nature* 349:482–487.

Smit J. 1999. The global stratigraphy of the Cretaceous-Tertiary boundary impact ejecta. *Annual Review of Earth and Planetary Science* 27:75–113.

Smit J. and Hertogen J. 1980. An extraterrestrial event at the Cretaceous-Tertiary boundary. *Nature* 285:198–200.

Smit J. and Klaver G. 1981. Sanidine spherules at the Cretaceous-Tertiary boundary indicate a large impact event. *Nature* 292:47–49.

Smit J. and Kyte F. T. 1984. Siderophile-rich magnetic spheroids from the Cretaceous-Tertiary boundary in Umbria, Italy. *Nature* 310:403–405.

Smit J. and Ten Kate W. G. H. Z. 1982. Trace element patterns at the Cretaceous-Tertiary boundary—Consequences of a large impact. *Cretaceous Research* 3:307–332.

Smit J., Montanari A., Swinburne N. H. M., Alvarez W., Hildebrand A. R., Margolis S. V., Claeys Ph., Lowrie W., and Asaro F. 1992. Tektite-bearing, deep-water clastic unit at the Cretaceous-Tertiary boundary in northeastern Mexico. *Geology* 20:99–103.

Smit J., Roep Th. B., Alvarez W., Montanari A., Claeys Ph., Grajales-Nishimura J. M., and Bermudez J. 1996. Coarse-grained, clastic sandstone complex at the K/T boundary around the Gulf of Mexico: Deposition by tsunami waves induced by the Chicxulub impact? In *The Cretaceous-Tertiary boundary event and other catastrophes in Earth history*, edited by Ryder G., Fastovsky D., and Gartner S. GSA Special Paper #307. Boulder, Colorado: Geological Society of America. pp. 151–182.

Smit J., Rocchia R., Robin E., and Odp Leg 171b Shipboard Party. 1997. Preliminary iridium analyses from a graded spherule layer at the K-T boundary and late Eocene ejecta from ODP Sites 1049, 1052, 1053, Blake Nose, Florida. *GSA Abstracts with Programs* 29:A141.

Soria A. R., Liesa C. L., Mata M. P., Arz J. A., Alegret L., Arenillas I., and Melendez A. 2001. Slumping and sandbar deposit at the Cretaceous-Tertiary boundary in the Ell Tecolote section (northeastern Mexico): An impact-induced sediment gravity flow. *Geology* 29:231–234.

Stinnesbeck W., Barbarin J. M., Keller G., Lopez-Oliva J. G., Pivnik D. A., Lyons J. B., Officer C. B., Adatte T., Graup G., Rocchia R., and Robin E. 1993. Deposition of channel deposits near the Cretaceous-Tertiary boundary in northeastern Mexico: Catastrophic or "normal" sedimentary deposits? *Geology* 21: 797–800.

Swisher C. C. III, Grajales-Nishimura J. M., Montanari A., Margolis S. V., Claeys P., Alvarez W., Renne P., Cedillo-Pardoa E., Maurrasse F. J-M. R., Curtis G. H., Smit J., and McWilliams M. O. 1992. Coeval $^{40}Ar/^{39}Ar$ ages of 65.0 million years ago from Chicxulub crater melt rock and Cretaceous-Tertiary boundary tektites. *Science* 257:954–958.

Ten Kate W. G. H. Z. and Sprenger A. 1993. Orbital cyclicities above and below the Cretaceous/Paleogene boundary at Zumaya (N Spain), Agost and Relleu (SE Spain). *Sedimentary Geology* 87: 69–101.

Turekian K. K. 1982. Potential of $^{187}Os/^{186}Os$ as a cosmic versus terrestrial indicator in high iridium layers of sedimentary strata. In *Geological implications of impacts and large asteroids and comets on the Earth*, edited by Silver L. T. and Schultz P. H. GSA Special Paper #190. Boulder, Colorado: Geological Society of America. pp. 243–249.

Verma H. C., Upadhyay C., Tripathi R. P., Tripathi A., Shukla A. D., and Bhandari N. 2001. Nano-sized iron phases at the K/T and P/T boundaries revealed by Mössbauer spectroscopy. LPI Contribution #1270. Houston, Texas: Lunar and Planetary Institute.

Wdowiak T. J., Armendarez L. P., Agresti D. G., Wade M. L., Wdowiak S. Y., Claeys Ph., and Izett G. 2001. Presence of an iron-rich nanophase material in the upper layer of the Cretaceous-Tertiary boundary clay. *Meteoritics & Planetary Science* 36:123–133.

Worm H. U. and Banerjee S. K. 1987. Rock magnetic signature of the Cretaceous-Tertiary boundary. *Geophysical Research Letters* 14: 1083–1086.